Gradient Algorithms for Complex Non-Gaussian Independent Component/Vector Extraction

Zbyněk Koldovský 1 and Petr Tichavský 2

¹Acoustic Signal Analysis and Processing Group, Faculty of Mechatronics, Informatics, and Interdisciplinary

Studies, Technical University of Liberec, Studentská 2, 461 17 Liberec, Czech Republic.

E-mail: zbynek.koldovsky@tul.cz, fax:+420-485-353112, tel:+420-485-353534

²The Czech Academy of Sciences, Institute of Information Theory and Automation,
Pod vodárenskou věží 4, P.O. Box 18, 182 08 Praha 8, Czech Republic. E-mail:
tichavsk@utia.cas.cz, fax:+420-2-868-90300, tel. +420-2-66052292

Abstract

We address the problem of extracting one independent component from an instantaneous linear mixture of signals. Compared to Independent Component Analysis, a novel parameterization of the mixing model is used. Our statistical model is based on the non-Gaussianity of the source of interest, while the other background signals are assumed to be Gaussian. Three gradient-based estimation algorithms are derived using the maximum likelihood principle. These ideas and algorithms are also generalized for the extraction of a vector component when the extraction proceeds jointly from a set of instantaneous mixtures. In simulations, we mainly focus on the size of the region of convergence for which the algorithms guarantee the extraction of the desired source. The proposed methods show superior results under various levels of initial signal-to-interference ratio, in comparison with state-of-the-art algorithms. The computational complexity of the proposed algorithms grows linearly with the number of channels.

Index Terms

Blind Source Separation, Blind Source Extraction, Independent Component Analysis, Independent Vector Analysis

I. INTRODUCTION

A. Independent Component Analysis

Independent Component Analysis has been a popular method studied for Blind Source Separation since the 1990s [1], [2], [3], [4]. In the basic ICA model, signals observed on d sensors are assumed to be linear mixtures

⁰Part of this paper was presented at the 25th European Signal Processing Conference (EUSIPCO 2017) in Kos, Greece. This work was supported by The Czech Science Foundation through Project No. 17-00902S.

of d "original" signals, which are mutually independent in the statistical sense. The mixing model is given by

$$\mathbf{x}(n) = \mathbf{A}\mathbf{u}(n),\tag{1}$$

where $\mathbf{x}(n)$ is a $d \times 1$ vector of the mixed signals; \mathbf{A} is a $d \times d$ nonsingular mixing matrix; $\mathbf{u}(n)$ is a $d \times 1$ vector of the original signals; and n denotes the sample index. In the non-Gaussianity-based ICA, the jth original signal $u_j(n)$ (the jth element of $\mathbf{u}(n)$) is modeled as an independently and identically distributed (i.i.d.) sequence of random variables with the probability density function (pdf) $p_j(\cdot)$. Our goal is to estimate \mathbf{A}^{-1} using $\mathbf{x}(n)$, $n=1,\ldots,N$, through finding a square de-mixing matrix \mathbf{W} such that $\mathbf{y}(n)=\mathbf{W}\mathbf{x}(n)$ are independent or as close to independent as possible. In the discussion that follows, we will omit the sample index n for the sake of brevity, except where it is required.

While our focus in this paper is on complex-valued signals and parameters, our conclusions are valid for the real-valued case as well.

B. The Extraction of One Independent Source

This work addresses the problem of extraction (separation) of one independent component, which is often sufficient in applications such as speaker source enhancement, passive radar and sonar, or in biomedical signal processing. The complete decomposition performed by ICA can be computationally very demanding and superfluous. This is especially remarkable when there is a large number of sensors (say, 10 or more), or when a large number of mixtures (say, 128 or more) are separated in parallel, as in the Frequency-Domain ICA (FD-ICA) [5]. The idea of extracting only one source can also be applied in joint BSS [6], [7], [8], especially in Independent Vector Analysis (IVA) [9]. Here, the "source" is represented by a vector of separated components from the mixtures that are mutually dependent (but independent of the other vector components).

In practice, the separation of one source is rarely solved as a purely blind problem. Indeed, some partial knowledge must be available that allows us to determine which source in the mixture is of our particular interest, as ICA involves the permutation ambiguity [2], [10]. For example, the a priori knowledge could be an expected direction of arrival (DOA) of the source, location of the source within a confined area [11], a property such as dominance within an angular range [12] or temporal structure [13], and so forth. Throughout this paper, we will consider cases where such knowledge is available and can be transformed into an initial value of a (de)mixing parameter. The wanted signal will be referred to as *source of interest (SOI)* while the rest of the mixture will be referred to as *background*.

The theoretical part of this paper will be constrained to the determined case, that is, when there is the same number of the mixed signals, d, as that of the original signals. This assumption need not be overly restrictive when only one source should be extracted. Indeed, when the mixture \mathbf{x} consists of more than d sources (underdetermined case), algorithms based on the determined model can still be used provided that they are sufficiently robust against mismodeling and noise. For example, the determined model was applied to separating dominant speakers in [14].

C. State-of-the-Art

The blind separation of one particular source has already been studied in several contexts and some authors refer to it as Blind Signal Extraction (BSE) [15], [16], [13]. Projection pursuit [17], a technique used for exploratory data analysis, aims at finding "interesting" projections, including 1-D signals. This "interestingness" is defined through various measures reflecting the distance of the projected signal's pdf from the Gaussian distribution [2], [18]. Various criteria of the interestingness were also derived in other contexts. For example, kurtosis appears in methods for blind adaptive beamforming or as a higher-order cumulant-based contrast; see, e.g., [19], [20], [21].

This framework was unified under ICA based on information theory [22]. Namely, the independence of signals can be measured using mutual information, which is the Kullback-Leibler divergence between the joint density of signals and the product of their marginal densities. The signals are independent if and only if that mutual information equals zero. Provided that $\mathbf{x}(t)$ are not correlated, the mutual information of $\mathbf{y}(n)$ is equal to the sum of entropies of $y_1(n), \ldots, y_d(n)$, up to a constant. Hence, it follows that an independent component can be sought through minimizing the entropy of the separated signal under the constraint $\mathbf{E}[|\mathbf{w}^H\mathbf{x}|^2] = 1$; here $\mathbf{E}[\cdot]$ stands for the expectation operator; and \mathbf{w}^H is a de-mixing vector (a row of the de-mixing matrix \mathbf{W}). The fact that entropy is a measure of non-Gaussianity reveals the connection between the ICA-based separation of one signal and the contrast-based techniques [2], [23].

In fact, many ICA methods apply d BSE estimators sequentially [24] or in parallel [25] to find all independent components in the mixture. The orthogonal constraint, which requires that the sample correlation between separated signals is equal to zero, is imposed on the BSE outputs in order to prevent the algorithms from finding any components twice. For example, the well-known FastICA algorithm has three basic variants: One-Unit FastICA is a BSE method optimizing the component's non-Gaussianity [26]; Deflation FastICA applies the one-unit version sequentially [27]; Symmetric FastICA runs d one-unit algorithms simultaneously [27], [28].

The separation accuracy of the above methods is known to be limited [29]. One-unit FastICA exploits only the non-Gaussianity of SOI and does not use the non-Gaussianity of the background [30]. The accuracy levels of deflation and symmetric FastICA are limited due to the orthogonal constraint [31]. While the latter limitation can be overcome, as shown, e.g., in [32], the limited accuracy of the one-unit approach poses an open problem, unless the BSE is done through the complete ICA. By comparing the performance analyses from [30], [33], [29] and the Cramér-Rao bound for ICA [32], it follows that one-unit methods can approach the optimum performance only when the background is Gaussian, but not otherwise.

D. Contribution

In this paper, we revisit the BSE problem by considering it explicitly as the goal to extract one component from the instantaneous mixture that is as close to being independent of the background as possible; we refer to this approach as *Independent Component Extraction (ICE)*. A novel parameterization of the mixing model (1) is introduced. Then, a statistical model is adopted from the non-Gaussianity-based ICA where the background is assumed to be Gaussian. The classical maximum likelihood estimation of the mixing parameters is considered,

by which a simplistic gradient-based estimation algorithm is derived. Our derivation provides a deeper insight into the BSE problem. We point to the roles of both the orthogonal constraint and the background's pdf.

For the practical output of this paper, we focus on the region of convergence (ROC) of the BSE algorithms. This aspect is important when extracting the SOI using an initial guess. The desired property of a BSE method is that it extracts the SOI with as little sensitivity to the initial bias as possible. The size of the ROC is dependent on the initial Signal-to-Interference Ratio (SIR), as it has a high influence on the shape of the contrast function. Our experiments show that the size of ROC and the speed of convergence of the gradient algorithm depend on whether the optimization proceeds in the mixing or de-mixing parameter. Based on this, we propose a novel variant where the optimization parameter is selected automatically, which combines advantages found in both variants.

Finally, the above ideas are generalized to the extraction of vector components, so-called *Independent Vector Extraction (IVE)*. Here, the problem defines several instantaneous mixtures to be treated simultaneously using joint statistical models. The goal is to extract one independent component in each mixture, where these components should be as dependent as possible. In other words, IVE is an extension of ICE similar to that of ICA to IVA [34], [35]. A gradient algorithm with automatic selection of the optimization parameter is derived, similar to that for ICE. Results of a simulation study prove good convergence behavior in terms of the size of ROC in comparison to other methods, especially when the background is non-Gaussian.

The rest of this paper is organized as follows. Section II introduces algebraic and statistical models for ICE. Section III is devoted to gradient-based ICE algorithms. The ideas and algorithms are generalized to the extraction of vector components in Section IV. Section V presents results of extensive simulations, and Section VI concludes the paper.

II. INDEPENDENT COMPONENT EXTRACTION

Nomenclature: The following notation will be used throughout the article. Plain letters denote scalars, bold lower-case letters denote vectors, and bold capital letters denote matrices. The Matlab conventions for matrix/vector concatenation and indexing will be used, e.g., $[1; \mathbf{g}] = [1, \mathbf{g}^T]^T$, and $(\mathbf{A})_{j,:}$ is the jth row of \mathbf{A} . Next, \mathbf{g}^T , $\overline{\mathbf{g}}$, and \mathbf{g}^H denote the transpose, the complex conjugate value and the conjugate transpose of \mathbf{g} , respectively. Symbolic scalar and vector random variables will be denoted by lower-case letters, e.g., s and s, while the quantities collecting their s samples will be denoted by bold (capital) letters, e.g., s and s. Estimated values of signals will be denoted by hats, e.g., s. For simplicity, the hat will be omitted in the case of estimated values of parameters, e.g., s, unless it is necessary to distinguish between its estimated and true values.

A. Mixing Model Parameterization

Without any loss of generality, let the SOI be $s = u_1$ and a be the first column of A, so it can be partitioned as $A = [a, A_2]$. Then, x can be written in the form

$$\mathbf{x} = \mathbf{a}s + \mathbf{y},\tag{2}$$

where $\mathbf{y} = \mathbf{A}_2 \mathbf{u}_2$ and $\mathbf{u}_2 = [u_2, \dots, u_d]^T$. The single-target description (2) has been widely studied in array processing literature [36]. Here, the fact that $\mathbf{y} = \mathbf{A}_2 \mathbf{u}_2$ means that we restrain our considerations to the determined scenario (the mixture consists of the same number of sources as that of the sensors).

Let the new mixing matrix for ICE and its inverse matrix be denoted by $\mathbf{A}_{\rm ICE}$ and $\mathbf{W}_{\rm ICE}$, respectively. In ICE, the identification of \mathbf{A}_2 or the decomposition of \mathbf{y} into independent signals is *not* the goal. Therefore, the structure of the mixing matrix is $\mathbf{A}_{\rm ICE} = [\mathbf{a}, \mathbf{Q}]$ where \mathbf{Q} is, for now, arbitrary.

Then, (2) can be written as

$$\mathbf{x} = \mathbf{A}_{\text{ICE}}\mathbf{v},\tag{3}$$

where $\mathbf{v} = [s; \mathbf{z}]$, and $\mathbf{y} = \mathbf{Q}\mathbf{z}$. It holds that \mathbf{z} spans the same subspace as that spanned by \mathbf{u}_2 .

To complete the mixing model definition, we look at the inverse matrix $\mathbf{W}_{\rm ICE} = \mathbf{A}_{\rm ICE}^{-1}$. Let \mathbf{a} and $\mathbf{W}_{\rm ICE}$ be partitioned, respectively, as

$$\mathbf{a} = \begin{pmatrix} \gamma \\ \mathbf{g} \end{pmatrix} \tag{4}$$

and

$$\mathbf{W}_{\text{ICE}} = \begin{pmatrix} \mathbf{w}^H \\ \mathbf{B} \end{pmatrix}. \tag{5}$$

B is required to be orthogonal to a, i.e., $\mathbf{Ba} = \mathbf{0}$, which ensures that the signals separated by the lower part of \mathbf{W}_{ICE} , namely, by \mathbf{Bx} , do not contain any contribution of s. A useful selection is

$$\mathbf{B} = \begin{pmatrix} \mathbf{g} & -\gamma \mathbf{I}_{d-1} \end{pmatrix},\tag{6}$$

where I_d denotes the $d \times d$ identity matrix. Let w be partitioned as

$$\mathbf{w} = \begin{pmatrix} \beta \\ \mathbf{h} \end{pmatrix}. \tag{7}$$

The de-mixing matrix then has the structure

$$\mathbf{W}_{\text{ICE}} = \begin{pmatrix} \mathbf{w}^H \\ \mathbf{B} \end{pmatrix} = \begin{pmatrix} \overline{\beta} & \mathbf{h}^H \\ \mathbf{g} & -\gamma \mathbf{I}_{d-1} \end{pmatrix}, \tag{8}$$

and from $\mathbf{A}_{\mathrm{ICE}}^{-1} = \mathbf{W}_{\mathrm{ICE}}$ it follows that

$$\mathbf{A}_{\text{ICE}} = \begin{pmatrix} \mathbf{a} & \mathbf{Q} \end{pmatrix} = \begin{pmatrix} \gamma & \mathbf{h}^{H} \\ \mathbf{g} & \frac{1}{\gamma} \left(\mathbf{g} \mathbf{h}^{H} - \mathbf{I}_{d-1} \right) \end{pmatrix}, \tag{9}$$

where β and γ are linked through

$$\overline{\beta}\gamma = 1 - \mathbf{h}^H \mathbf{g}. \tag{10}$$

The latter equation can also be written in the form $\mathbf{w}^H \mathbf{a} = 1$, which is known as the *distortionless response* constraint; see page 515 in [36].

It is worth mentioning here that ICE and Multidimensional ICA [37] are similar to each other; the latter is also known as Independent Subspace Analysis (ISA) [38]. In ISA, the goal is to separate subspaces of components that are mutually independent while components inside of the subspaces can be dependent. The goal to separate one independent component thus could be formulated as a special case of ISA where **u** is

divided into two subspaces of dimensions 1 and d-1, respectively. What makes ICE different is that the separation of the background subspace from the SOI is not as ambiguous as in ISA, which is ensured by the structure of the de-mixing matrix.

The free variables in the ICE mixing model are the elements of \mathbf{g} and \mathbf{h} , and one of the parameters β or γ . In total, there are 2d-1 free (real or complex) parameters. The role of \mathbf{a} , as follows from (2), is the *mixing* vector related to s, which is in beamforming literature also sometimes referred to as the steering vector. Next, \mathbf{w} is the separating vector as $s = \mathbf{w}^H \mathbf{x}$. For the background signal \mathbf{z} , it holds that

$$z = Bx = By = BA_2u_2. \tag{11}$$

Note that A_2 is not identified in the model, so the relationship between z and u_2 remains unknown after performing ICE. The components of z are independent after the extraction only when d=2 or, for d>2, in very special cases that $BA_2 = \Lambda P$; Λ denotes a diagonal (scaling) matrix with non-zero elements on the main diagonal, and P denotes a permutation matrix.

B. Indeterminacies

Similarly to ICA, the scales of s and of a are ambiguous in the sense that, in (2) they can be replaced, respectively, by αs and $\alpha^{-1}a$ where $\alpha \neq 0$. The scaling ambiguity can be avoided by fixing β or γ . A specific case occurs when $\gamma = 1$ [39], since then s corresponds to the so-called spatial image of the SOI on the first sensor [40], [41], [42]. This can be useful for modeling the pdf of s, as the physical meaning of that scale is often known. By contrast, when no such knowledge is given, it might be better to keep γ (or β) free.

The second ambiguity is that the role of $s = u_1$ is interchangeable with any independent component of x, that is, with any u_i , i = 2, ..., d. This fact is known as the permutation problem [23], [43] in BSS. As was already stated, in this work we assume that an initial guess of either a or w is given.

C. Statistical Model

The main principle of ICE is the same as that of ICA. We make the assumption that s and \mathbf{z} are *independent*, and ICE is formulated as follows:

Find vectors \mathbf{a} and \mathbf{w} such that $\mathbf{w}^T \mathbf{x}$ and $\mathbf{B} \mathbf{x}$ are independent (or as close to independent as possible).

Let the pdf of s and of z be, respectively, denoted by $p_s(\xi_1)$ and $p_z(\xi_2)$; ξ_1 and ξ_2 denote free variables of appropriate dimensions. The joint pdf of s and z is, owing to their mutual independence,

$$p_{\mathbf{s}}(\boldsymbol{\xi}) = p_s(\xi_1) \cdot p_{\mathbf{z}}(\boldsymbol{\xi}_2), \tag{12}$$

where $\boldsymbol{\xi} = [\xi_1; \boldsymbol{\xi}_2]$. From (8), the joint pdf of the mixed signals $\mathbf{x} = \mathbf{A}_{ICE}\mathbf{v}$ is

$$p_{\mathbf{x}}(\boldsymbol{\xi}) = p_s(\mathbf{w}^H \boldsymbol{\xi}) \cdot p_{\mathbf{z}}(\mathbf{B}\boldsymbol{\xi}) \cdot |\det \mathbf{W}_{ICE}|^2$$
(13)

$$= p_s(\overline{\beta}\xi_1 + \mathbf{h}^H \boldsymbol{\xi}_2) \cdot p_{\mathbf{z}}(\xi_1 \mathbf{g} - \gamma \boldsymbol{\xi}_2) \cdot |\gamma|^{2(d-2)}, \tag{14}$$

where the identity

$$\det \mathbf{W}_{\text{ICE}} = (-1)^{d-1} \gamma^{d-2} \tag{15}$$

$$= (-1)^{d-1} \beta^{-(d-2)} (1 - \mathbf{h}^H \mathbf{g})^{d-2}, \tag{16}$$

was used, which can easily be verified from (8) using (10).

The log-likelihood function of N signal samples depends on a and w; hence it is

$$\mathcal{L}(\mathbf{a}, \mathbf{w}) = \frac{1}{N} \log \prod_{n=1}^{N} p_{\mathbf{x}}(\mathbf{a}, \mathbf{w} | \mathbf{x}(n))$$

$$= \frac{1}{N} \sum_{n=1}^{N} \log p_{s}(\mathbf{w}^{H} \mathbf{x}(n)) + \frac{1}{N} \sum_{n=1}^{N} \log p_{\mathbf{z}}(\mathbf{B} \mathbf{x}(n))$$

$$+ (d-2) \log |\gamma|^{2}.$$
(18)

D. Gaussian Background

As previously explained in Section II-A, the background signals are highly probable to remain unmixed after ICE, unless d=2. This opens the problem of modeling the pdf of \mathbf{z} . A straightforward choice is that the components of \mathbf{z} have the circularly symmetric Gaussian distribution with zero mean and covariance $\mathbf{C}_{\mathbf{z}}$, i.e., $\mathbf{z} \sim \mathcal{CN}(\mathbf{0}, \mathbf{C}_{\mathbf{z}})$. This choice can be justified by the fact that the said components are mixed and correlated; moreover, from the Central Limit Theorem it follows that their distribution is close to Gaussian [23]. The covariance matrix $\mathbf{C}_{\mathbf{z}} = \mathrm{E}[\mathbf{z}\mathbf{z}^H]$ is a nuisance parameter.

In this paper, we restrain our considerations to this Gaussian background model, noting that other choices are worthy of future investigation. Hence, (18) takes the form

$$\mathcal{L}(\mathbf{a}, \mathbf{w}) = \frac{1}{N} \sum_{n=1}^{N} \log p_s(\mathbf{w}^H \mathbf{x}(n))$$
$$-\frac{1}{N} \sum_{n=1}^{N} \mathbf{x}(n)^H \mathbf{B}^H \mathbf{C}_{\mathbf{z}}^{-1} \mathbf{B} \mathbf{x}(n) + (d-2) \log |\gamma|^2$$
$$-\log \det \mathbf{C}_{\mathbf{z}} - d \log \pi. \quad (19)$$

E. Orthogonal Constraint

By inspecting (18) and (19), it can be seen that the link between a and w, which are both related to the SOI, is rather "weak". Indeed, the first term on the right-hand side of (18) depends purely on w, while the second and the third terms depend purely on a. The only link between a and w is thus expressed in (10). Consequently, the log-likelihood function can have spurious maxima where a and w do not jointly correspond to the SOI.

Many ICA algorithms impose the orthogonal constraint (OG) [31], which decreases the number of unknown parameters in the mixing model. This constraint can be used to avoid spurious solutions in ICE and to stabilize the convergence of algorithms. Let now $\mathbf{W}_{\rm ICE}$ denote an ICE de-mixing matrix estimate and

$$\widehat{\mathbf{V}} = \begin{pmatrix} \widehat{\mathbf{s}} \\ \widehat{\mathbf{Z}} \end{pmatrix} = \mathbf{W}_{\text{ICE}} \mathbf{X}$$
 (20)

be the estimated de-mixed signals. The OG means that

$$\frac{1}{N}\widehat{\mathbf{s}} \cdot \widehat{\mathbf{Z}}^{H} = \frac{1}{N} \mathbf{w}^{H} \mathbf{X} \mathbf{X}^{H} \mathbf{B}^{H} = \mathbf{w}^{H} \widehat{\mathbf{C}}_{\mathbf{x}} \mathbf{B}^{H} = \mathbf{0},$$
(21)

where $\widehat{\mathbf{C}}_{\mathbf{x}} = \mathbf{X}\mathbf{X}^H/N$ is the sample-based estimate of $\mathbf{C}_{\mathbf{x}} = \mathrm{E}[\mathbf{x}\mathbf{x}^H]$.

The OG introduces a link between a and w, so $W_{\rm ICE}$ is a function of either a or w. The dependencies, whose derivations are given in Appendix A, are

$$\mathbf{w} = \frac{\widehat{\mathbf{C}_{\mathbf{x}}}^{-1} \mathbf{a}}{\mathbf{a}^{H} \widehat{\mathbf{C}_{\mathbf{x}}}^{-1} \mathbf{a}},\tag{22}$$

when a is the dependent variable, and

$$\mathbf{a} = \frac{\widehat{\mathbf{C}}_{\mathbf{x}} \mathbf{w}}{\mathbf{w}^H \widehat{\mathbf{C}}_{\mathbf{x}} \mathbf{w}},\tag{23}$$

when the dependent variable is w.

Interestingly, the coupling (22) corresponds to the approximation of

$$\mathbf{w}_{\mathrm{MPDR}}^{H}\mathbf{x} = \frac{\mathbf{a}^{H}\mathbf{C}_{\mathbf{x}}^{-1}}{\mathbf{a}^{H}\mathbf{C}_{\mathbf{x}}^{-1}\mathbf{a}}\mathbf{x}.$$
 (24)

The minimum-power distortionless (MPDR) beamformer is thus steered in the direction given by **a**, the well-known optimum beamformer in array processing theory [36]; see also [39]. In Appendix B, it is shown that if **a** is equal to its true value, then

$$\mathbf{w}_{\mathrm{MPDR}}^{H}\mathbf{x} = s. \tag{25}$$

The advantage of (23) is that the computation of a does not involve the inverse of \widehat{C}_x .

III. GRADIENT-BASED ICE ALGORITHMS

In this section, we derive gradient ICE algorithms aiming at the maximum likelihood estimation through searching for the maximum of (19). Since p_s and C_z in (19) are not known, we propose a contrast function replacing the true one where p_s and C_z are approximated in a certain way. This is sometimes referred to as the quasi-maximum likelihood approach; see, e.g., [44].

We present two variants constrained by the OG performing the optimization, respectively, in variable w and a. The former variant shows stable and fast convergence when the input ISR is "low", while the latter variant has exactly the opposite qualities. Based on this, we propose a novel method that automatically selects the better optimization strategy.

A. Optimization in w

For the optimization in w, given the coupling (23), β is selected as a free variable while γ is dependent. Following (19), the contrast function is defined as

$$C(\mathbf{a}, \mathbf{w}) = \frac{1}{N} \sum_{n=1}^{N} \left\{ \log f(\mathbf{w}^H \mathbf{x}(n)) - \mathbf{x}(n)^H \mathbf{B}^H \mathbf{R} \mathbf{B} \mathbf{x}(n) \right\} + (d-2) \log |\gamma|^2,$$
(26)

where $f(\cdot)$ is the model pdf of the target signal (replacing p_s), and \mathbf{R} is a weighting positive definite matrix (replacing $\mathbf{C}_{\mathbf{z}}^{-1}$).

Using the Wirtinger calculus [45], [46], we derive in Appendix C that the gradient of \mathcal{C} with respect to \mathbf{w}^H , under the coupling (23), equals

$$\frac{\partial \mathcal{C}}{\partial \mathbf{w}^{H}} \bigg|_{\mathbf{w.r.t.} (23)} = -\frac{1}{N} \mathbf{X} \phi(\mathbf{w}^{H} \mathbf{X})^{T} + 2\mathbf{a} \operatorname{tr}(\mathbf{R} \widehat{\mathbf{C}}_{\mathbf{z}})
- (\mathbf{w}^{H} \widehat{\mathbf{C}}_{\mathbf{x}} \mathbf{w})^{-1} (\widehat{\mathbf{C}}_{\mathbf{x}} \mathbf{E}^{H} \mathbf{R} \widehat{\mathbf{C}}_{\mathbf{z}} \mathbf{h} - \operatorname{tr}(\mathbf{R} \mathbf{B} \widehat{\mathbf{C}}_{\mathbf{x}} \mathbf{E}^{H}) \widehat{\mathbf{C}}_{\mathbf{x}} \mathbf{e}_{1})
- 2(d - 2)\mathbf{a} + \overline{\gamma}^{-1} (d - 2) (\mathbf{w}^{H} \widehat{\mathbf{C}}_{\mathbf{x}} \mathbf{w})^{-1} \widehat{\mathbf{C}}_{\mathbf{x}} \mathbf{e}_{1}, \quad (27)$$

where $tr(\cdot)$ denotes the trace; $\mathbf{E} = [\mathbf{0} \ \mathbf{I}_{d-1}]; \mathbf{e}_1$ denotes the first column of \mathbf{I}_d ; and

$$\phi(\xi) = -\frac{\partial \log f(\xi)}{\partial \xi} \tag{28}$$

is the score function of the model pdf $f(\cdot)$.

Now, we put $\mathbf{R} = \widehat{\mathbf{C}}_{\mathbf{z}}^{-1}$; this is a choice for which the derivative of (19) with respect to the unknown parameter $\mathbf{C}_{\mathbf{z}}$ is equal to zero. Then, the following identities can be applied in (27).

$$\operatorname{tr}(\widehat{\mathbf{C}}_{\mathbf{z}}^{-1}\widehat{\mathbf{C}}_{\mathbf{z}}) = \operatorname{tr}(\mathbf{I}_{d-1}) = d - 1, \tag{29}$$

$$\mathbf{E}^H \mathbf{h} + \beta \mathbf{e}_1 = \mathbf{w},\tag{30}$$

$$\widehat{\mathbf{C}}_{\mathbf{z}}^{-1}\mathbf{B}\widehat{\mathbf{C}}_{\mathbf{x}} = \widehat{\mathbf{C}}_{\mathbf{z}}^{-1}\mathbf{B}\mathbf{X}\mathbf{X}^{H}/N$$

$$= \widehat{\mathbf{C}}_{\mathbf{z}}^{-1}\widehat{\mathbf{Z}}[\widehat{\mathbf{s}}^{H} \ \widehat{\mathbf{Z}}^{H}]\mathbf{A}_{\text{ICE}}^{H} = \mathbf{E}\mathbf{A}_{\text{ICE}}^{H}$$
(31)

$$\operatorname{tr}(\widehat{\mathbf{C}}_{\mathbf{z}}^{-1}\mathbf{B}\widehat{\mathbf{C}}_{\mathbf{x}}\mathbf{E}^{H}) = \operatorname{tr}(\mathbf{E}\mathbf{A}_{\text{ICE}}^{H}\mathbf{E}^{H}) =$$

$$= \overline{\gamma}^{-1}\operatorname{tr}(\mathbf{h}\mathbf{g}^{H} - \mathbf{I}_{d-1}) =$$

$$= -\beta - (d-2)\overline{\gamma}^{-1},$$
(32)

where we used (20) and (21); (27) is now simplified to

$$\left. \frac{\partial \mathcal{C}}{\partial \mathbf{w}^H} \right|_{\text{w.r.t. (23)}} = \mathbf{a} - \frac{1}{N} \mathbf{X} \phi(\mathbf{w}^H \mathbf{X})^T.$$
 (33)

In fact, $\mathbf{R} = \widehat{\mathbf{C}}_{\mathbf{z}}^{-1}$ depends on the current value of \mathbf{w} since $\widehat{\mathbf{C}}_{\mathbf{z}} = \mathbf{B}\widehat{\mathbf{C}}_{\mathbf{x}}\mathbf{B}^H$. It means that, with any estimate of \mathbf{w} , the distribution of $\widehat{\mathbf{Z}} = \mathbf{B}\mathbf{X}$ is assumed to be $\mathcal{CN}(\mathbf{0},\widehat{\mathbf{C}}_{\mathbf{z}})$, which obviously introduces little (or no) information into the contrast function. $\widehat{\mathbf{C}}_{\mathbf{z}}$ is close to the true covariance $\mathbf{C}_{\mathbf{z}}$ only when \mathbf{a} is close to its true value.

For $N \to +\infty$, (33) takes on the form

$$\frac{\partial \mathcal{C}}{\partial \mathbf{w}^H} = \mathbf{a} - \mathbf{E}[\mathbf{x}\phi(\mathbf{w}^H\mathbf{x})]. \tag{34}$$

When w is the ideal separating vector, that is, when $\mathbf{w}^H\mathbf{x} = s$, then from (2) it follows that

$$\frac{\partial \mathcal{C}}{\partial \mathbf{w}^H} = (1 - \mathbf{E}[s\phi(s)])\mathbf{a}. \tag{35}$$

This shows us that the true separating vector is a stationary point of the contrast function only if $\phi(\cdot)$ satisfies the condition

$$E[s\phi(s)] = 1. (36)$$

Based on this observation, we propose a method whose steps are described in Algorithm 1. In every step, it iterates in the direction of the steepest ascent of \mathcal{C} where $\mathbf{R} = \widehat{\mathbf{C}}_{\mathbf{z}}^{-1}$ (step 9), and $\phi(\cdot)$ is normalized so that condition (36) is satisfied for the current target signal estimate $\widehat{s} = \mathbf{w}^H \mathbf{x}$ (see step 7). This is repeated until the norm of the gradient is smaller than tol; μ is the step length parameter; and \mathbf{w}_{ini} is the initial guess. We call this method OGICE_w.

When the observations X are preprocessed (whitened) so that $\widehat{C}_x = I_d$, steps 4 and 5 in Algorithm 1 are simplified to

$$\mathbf{a} \leftarrow \mathbf{w}/\|\mathbf{w}\|^2$$
.

Algorithm 1: $OGICE_{\mathbf{w}}$: separating vector estimation based on orthogonally constrained gradient-ascent algorithm

In fact, (34) coincides with the gradient of a heuristic criterion derived from mutual information in [33] (page 870, Eq. 4). The author, D.-T. Pham, called this approach "Blind Partial Separation". Our derivation provides a deeper insight into this result by showing its connection with maximum likelihood estimation. Most importantly, it is seen that (33) follows from a particular parameterization of the (de)-mixing model, it imposes the OG between $\bf a$ and $\bf w$, and it relies on the Gaussian modeling of the background signals whose covariance is estimated as $\hat{\bf C}_{\bf z}$.

B. Relation to gradient-based ICA methods

It is worth comparing OGICE_w with the method by Bell and Sejnowski [47] for ICA, whose popular improvement is known as Amari's Natural Gradient (NG) algorithm [48]; see also [49] and [46] for the complex-

Algorithm 2: OGICE_a: mixing vector estimation based on orthogonally constrained gradient-ascent algorithm

```
Input: X, a_{ini}, \mu, tol
      Output: a, w
 1 \widehat{\mathbf{C}}_{\mathbf{x}} = \mathbf{X}\mathbf{X}^H/N;
 \mathbf{a}=\mathbf{a}_{\mathrm{ini}};
 3 repeat
             \lambda_{\mathbf{a}} \leftarrow (\mathbf{a}^H \widehat{\mathbf{C}}_{\mathbf{x}}^{-1} \mathbf{a})^{-1};
         \mathbf{w} \leftarrow \lambda_{\mathbf{a}} \widehat{\mathbf{C}}_{\mathbf{x}}^{-1} \mathbf{a};
                                                                                                                                                                                     /* OG constraint (22) */
         \widehat{\mathbf{s}} \leftarrow \mathbf{w}^H \mathbf{X};
              \mathbf{q} \leftarrow \phi(\widehat{\mathbf{s}})/(\widehat{\mathbf{s}}\phi(\widehat{\mathbf{s}})^T/N);
                                                                                                                                                                                                  /* to fulfil (36) */
          \Delta \leftarrow \mathbf{w} - \lambda_{\mathbf{a}} \widehat{\mathbf{C}}_{\mathbf{x}}^{-1} \mathbf{X} \mathbf{q}^T / N;
                                                                                                                                                                                                                         /* by (39) */
               \mathbf{a} \leftarrow \mathbf{a} + \mu \Delta;
                                                                                                                                                                                           /* gradient ascent */
10 until \|\Delta\| < \text{tol};
```

valued variant. In each step of the Bell and Sejnowski's method (BS), the whole de-mixing matrix is updated as

$$\Delta \mathbf{W} \leftarrow \mathbf{W}^{-H} - \overline{\phi(\mathbf{W}^H \mathbf{X})} \mathbf{X}^H / N. \tag{37}$$

After taking the conjugate transpose on both sides, and denoting $W^{-1} = A$, this update can be re-written as

$$\Delta \mathbf{W}^H \leftarrow \mathbf{A} - \mathbf{X}\phi(\mathbf{W}^H \mathbf{X})^T / N. \tag{38}$$

Now, the right-hand side of (33) corresponds to any row on the right-hand side of (38). However, the respective algorithms are different. In particular, $OGICE_{\mathbf{w}}$ exploits the orthogonal constraint, while BS is not constrained and updates the whole (de-)mixing matrix. It follows that the estimation of any row of \mathbf{W} is influenced by the other rows. Next, the nonlinearity in $OGICE_{\mathbf{w}}$ is normalized according to (36), while neither BS nor NG apply any normalization. From this perspective, $OGICE_{\mathbf{w}}$ appears to be most similar to the Scaled Natural Gradient algorithm (NGsc) proposed in [50], which is popular due to faster convergence as compared to the original NG.

C. Optimization in a

The gradient with respect to a when ${\bf w}$ is dependent through (22) and when $\gamma=1$ has been derived in [39]. Treating γ as a free variable, and by putting ${\bf R}=\widehat{\bf C}_{\bf z}^{-1}$, the gradient reads

$$\frac{\partial \mathcal{C}}{\partial \mathbf{a}^H}\bigg|_{\mathbf{wrt}} = \mathbf{w} - \frac{\lambda_{\mathbf{a}}}{N} \widehat{\mathbf{C}}_{\mathbf{x}}^{-1} \mathbf{X} \phi(\mathbf{w}^H \mathbf{X})^T, \tag{39}$$

where $\lambda_{\mathbf{a}} = (\mathbf{a}^H \widehat{\mathbf{C}}_{\mathbf{x}}^{-1} \mathbf{a})^{-1}$. For $N \to +\infty$, the true mixing vector is a stationary point only if (36) is fulfilled. The corresponding algorithm, which will be referred to as OGICE_a, is described in Algorithm 2.

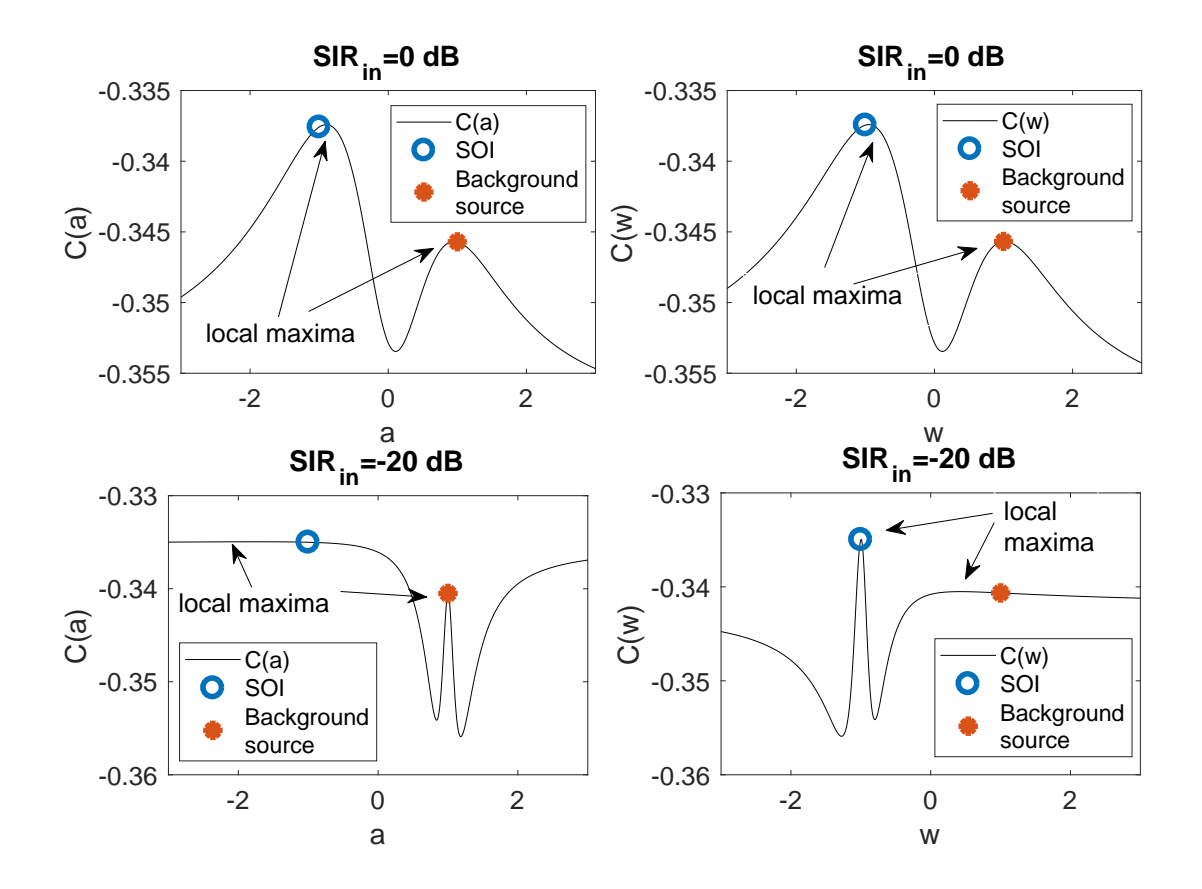


Fig. 1. Examples of the contrast function (26) as it depends on $\mathbf{a} = [1; a]$ and $\mathbf{w} = [1; w]$, respectively, for SIR_{in} is 0 dB and 20 dB.

D. Switched optimization

Without any loss of generality, let the initial Signal-to-Interference Ratio related to the SOI be defined as

$$SIR_{in} = \frac{E[|s|^2]}{\sum_{i=2}^{d} E[|u_i|^2]},$$
(40)

although a more precise definition also depends on the mixing matrix and the selected input channel. The following example shows how the performance of the above algorithms depends on ${\rm SIR_{in}}$.

Consider situation where s is a weak signal, i.e., $SIR_{in} \ll 0$ dB. The mixing vector \mathbf{a} is then hard to identify while the background subspace can be identified with high precision. For the de-mixing matrix, the problem is reciprocal. The estimation of \mathbf{B} in (8) is inaccurate as \mathbf{B} depends purely on \mathbf{a} , while the estimation of \mathbf{w} yields a low variance. SIR_{in} therefore has significant influence on the shape of the contrast function as well as on the size of the region of convergence (ROC) in the vicinity of the solution.

Fig. 1 shows the contrast function in the case of two real-valued Laplacean components (SOI and one background source) of the length N=1000; the mixing matrix is $\mathbf{A}=\begin{pmatrix} 1 & 1 \\ -1 & 1 \end{pmatrix}$; and $\mathrm{SIR}_{\mathrm{in}}$ is 0 dB and -20 dB, respectively. The contrast function (26) is shown as it depends on a and w, respectively, where the mixing vector is $\mathbf{a}=[1;a]$ and the separating vector is $\mathbf{w}=[1;w]$, respectively. The nonlinearity is $\log f(x)=-\log|\cosh(x/\sigma_x)|$ where σ_x^2 is the variance of the input. The ideal extraction of SOI is achieved for a=-1 and w=-1, while a=1 and w=1 correspond to the extraction of the background source.

For $SIR_{in} = 0$ dB, the dependencies on both a and w are almost the same. The local maxima are slightly

biased from ideal solutions, and the sizes of ROC related to the maxima are approximately equal for both sources. For $SIR_{in} = -20$ dB, the maximum corresponding to the mixing vector of the SOI is significantly biased from its ideal value, the function is almost flat in the vicinity of that maximum, and the corresponding ROC is wide. By contrast, the separating vector for SOI is precisely localized by a sharp local maximum, which has a narrow ROC. The exact opposite is true for the maxima corresponding to the dominating background source.

In conclusion, $OGICE_{\mathbf{w}}$ is more advantageous when $SIR_{in} \gg 0$ dB, since the ROC corresponding to the SOI is wide. When $OGICE_{\mathbf{w}}$ is initialized within the ROC, its convergence is faster as the gradient is steep enough. Similarly, $OGICE_{\mathbf{a}}$ is advantageous when $SIR_{in} \ll 0$ dB. These phenomena may not be visible through ICA methods, which estimate all sources (dominant and week) simultaneously.

Since SIR_{in} is not known in a blind scenario, we propose the following heuristic approach for the selection between the optimization in a and w. Let a be the current estimate of the mixing vector. Then,

$$\mathbf{b} = \widehat{\mathbf{C}}_{\mathbf{x}} \mathbf{a} \tag{41}$$

can be viewed as an approximate eigenvector of $\hat{\mathbf{C}}_{\mathbf{x}}$ corresponding to the largest eigenvalue. This eigenvalue is approximately equal to $\lambda_{\mathbf{b}} = b_1/a_1$. Thus, $\|\mathbf{a}/a_1 - \mathbf{b}/\lambda_{\mathbf{b}}\|$ is small when \mathbf{a} is close to the dominant eigenvector.

Next, to assess the dominance of that eigenvector, that is, whether it is significantly larger compared to the other eigenvectors, we propose to compute the ratio of norms of matrices $\hat{\mathbf{C}}_{\mathbf{x}} - \lambda_{\mathbf{b}} \mathbf{b} \mathbf{b}^H / \|\mathbf{b}\|^2$ and $\hat{\mathbf{C}}_{\mathbf{x}}$. The ratio is small when \mathbf{b} is a dominant eigenvector of $\hat{\mathbf{C}}_{\mathbf{x}}$. The criterion of "proximity and dominance" is therefore defined as

$$\mathcal{B}(\mathbf{a}) = \left\| \mathbf{a}/a_1 - \mathbf{b}/\lambda_{\mathbf{b}} \right\| \frac{\left\| \widehat{\mathbf{C}}_{\mathbf{x}} - \lambda_{\mathbf{b}} \mathbf{b} \mathbf{b}^H / \|\mathbf{b}\|^2 \right\|_F}{\| \widehat{\mathbf{C}}_{\mathbf{x}} \|_F}.$$
 (42)

The proposed algorithm, referred to as OGICE_s, selects the optimization parameter based on the current value of $\mathcal{B}(\mathbf{a})$. When $\mathcal{B}(\mathbf{a}) < \tau$, the optimization in \mathbf{w} is selected; otherwise, the optimization proceeds in \mathbf{a} . Normally, we select $\tau = 0.1$. To lower the computational load, the criterion is recomputed only once after Q iterations (Q = 10). The stopping condition of OGICE_s is the same as that in OGICE_w or OGICE_a; see the description in Algorithm 3.

IV. INDEPENDENT VECTOR EXTRACTION

A. Definition

In this section, we generalize the ideas for joint extraction of an independent vector component from a set of K instantaneous mixtures

$$\mathbf{x}^k = \mathbf{A}_{\text{ICE}}^k \mathbf{v}^k, \qquad k = 1, \dots, K. \tag{43}$$

Here, $\mathbf{A}_{\mathrm{ICE}}^k$ obeys the same structure as (3), and $\mathbf{v}^k = [s^k; \mathbf{z}^k]$. A joint mixture model can be written as

$$\mathbf{x} = \mathbf{A}_{\text{IVE}} \mathbf{v}. \tag{44}$$

The double-striked font will be used to denote concatenated variables or parameters from K mixtures, e.g., $\mathbf{x} = [\mathbf{x}^1; \dots; \mathbf{x}^K]$. The joint mixing matrix obeys $\mathbf{A}_{\mathrm{IVE}} = \mathtt{bdiag}(\mathbf{A}_{\mathrm{ICE}}^1, \dots, \mathbf{A}_{\mathrm{ICE}}^K)$, where $\mathtt{bdiag}(\cdot)$ denotes a block-diagonal matrix with the arguments on the main block-diagonal.

Algorithm 3: OGICEs: ICE algorithm with automatic selection of optimization parameter

```
Input: X, a_{ini}, \mu, tol, Q
      Output: a, w
 \widehat{\mathbf{C}}_{\mathbf{x}} = \mathbf{X}\mathbf{X}^H/N; \ \mathbf{a} = \mathbf{a}_{\mathrm{ini}}; \ i = 0;
              if i \equiv 0 \pmod{Q} then
                \kappa = \mathcal{B}(\mathbf{a});
                                                                                                                                                                                              /* using (42) */
 5
              i \leftarrow i + 1;
              if \kappa < 0.1 then
 7
                     Update w as in OGICEw
 8
               \mathbf{a} \leftarrow (\mathbf{w}^H \widehat{\mathbf{C}}_{\mathbf{x}} \mathbf{w})^{-1} \widehat{\mathbf{C}}_{\mathbf{x}} \mathbf{w};
10
                     Update a as in OGICE<sub>a</sub>
11
                     \mathbf{w} \leftarrow (\mathbf{a}^H \widehat{\mathbf{C}}_{\mathbf{x}}^{-1} \mathbf{a})^{-1} \widehat{\mathbf{C}}_{\mathbf{x}}^{-1} \mathbf{a};
12
              end
13
14 until \|\Delta\| < 	exttt{tol};
```

Although the mixtures $\mathbf{x}^1, \dots, \mathbf{x}^K$ are algebraically independent, similarly to IVA, we introduce a joint statistical model given by

$$p_{\mathbf{v}}(\mathbf{v}) = p_{\mathbf{s}}(\mathbf{s})p_{\mathbf{z}}(\mathbf{z}),\tag{45}$$

which means that s and z are independent but the elements inside of them can be dependent. Like in the previous section, we constrain our considerations to the Gaussian background modeling; so it is assumed that

$$\mathbf{z} \sim \mathcal{CN}(\mathbf{0}, \mathbf{C}_{\mathbf{z}}),$$
 (46)

where $\mathbf{C}_{\mathbf{z}} = \mathrm{E}[\mathbf{z}\mathbf{z}^H]$ whose ijth block of dimension $d-1\times d-1$ is $\mathbf{C}_{\mathbf{z}}^{ij} = \mathrm{E}[\mathbf{z}^i\mathbf{z}^j]$; similarly $\mathbf{C}_{\mathbf{x}}$ as well as the sample-based counterparts $\widehat{\mathbf{C}}_{\mathbf{z}}$ and $\widehat{\mathbf{C}}_{\mathbf{x}}$ are defined.

Similar to (26), the quasi-likelihood contrast function following from (45) (for one signal sample), is

$$\mathcal{J}(\mathbf{w}, \mathbf{a}) = \log f(\hat{s}^1, \dots, \hat{s}^K)$$

$$- \sum_{i=1}^K \sum_{j=1}^K \mathbf{x}^{iH} \mathbf{B}^{jH} \mathbf{R}^{ij} \mathbf{B}^j \mathbf{x}^j + \sum_{k=1}^K \log |\det \mathbf{W}_{\text{ICE}}^k|^2, \quad (47)$$

where $\hat{s}^k = (\mathbf{w}^k)^H \mathbf{x}^k$, and \mathbf{R}^{ij} is a weighting matrix substituting the ijth block of the unknown \mathbf{C}_z^{-1} .

B. Gradient of the contrast function

After a lengthy computation, which follows steps similar to those described in Appendix C (we skip the details to save space), the derivative of \mathcal{J} with respect to $(\mathbf{w}^k)^H$ under the constraints

$$\mathbf{a}^{k} = \frac{\widehat{\mathbf{C}}_{\mathbf{x}}^{kk} \mathbf{w}^{k}}{\mathbf{w}^{k} \widehat{\mathbf{C}}_{\mathbf{x}}^{kk} \mathbf{w}^{k}}, \quad k = 1, \dots, K,$$
(48)

and when $\mathbf{R}^{k\ell}$ is selected as the $k\ell$ th block of $\widehat{\mathbf{C}}_{z}^{-1}$, reads

$$\frac{\partial \mathcal{J}}{\partial \mathbf{w}^{kH}} = \mathbf{a}^{k} - \frac{1}{N} \mathbf{X}^{k} \phi^{k} (\hat{\mathbf{s}}^{1}, \dots, \hat{\mathbf{s}}^{K})^{T} + \frac{1}{\mathbf{w}^{kH} \hat{\mathbf{C}}_{\mathbf{x}}^{kk} \mathbf{w}^{k}} \hat{\mathbf{C}}_{\mathbf{x}}^{kk} \mathbf{B}^{kH} \boldsymbol{\epsilon}^{k}. \tag{49}$$

Here,
$$\hat{\mathbf{s}}^k = (\mathbf{w}^k)^H \mathbf{X}^k$$
,
$$\phi^k(\xi^1, \dots, \xi^K) = -\frac{\partial \log f(\xi^1, \dots, \xi^K)}{\partial \xi^k},$$
(50)

is the score function related to the model joint density $f(\cdot)$ of s with respect to the kth variable, and

$$\boldsymbol{\epsilon}^k = \sum_{\ell=1}^K \mathbf{R}^{k\ell} \boldsymbol{\theta}^{\ell k}, \text{ where } \boldsymbol{\theta}^{\ell k} = \widehat{\mathbf{Z}}^{\ell} (\widehat{\mathbf{s}}^k)^H / N.$$
(51)

By comparing (33) with (49), the latter differs only in that the nonlinearity $\phi^k(\cdot)$ is dependent on the SOI separated from all K mixtures, plus the third term that does not occur in (33).

 $\theta^{\ell k}$ is the sample correlation between the estimated SOI in the kth mixture and the separated background in the ℓ th mixture, and can also be written as $\theta^{\ell k} = \mathbf{B}^{\ell} \widehat{\mathbf{C}}_{\mathbf{x}}^{\ell k} \mathbf{w}^{k}$. For $k = 1, \ldots, K$, $\theta^{kk} = \mathbf{0}$ due to the OG, but, for $k \neq \ell$, $\theta^{\ell k}$ is non-zero in general. Therefore, the third term in (49) vanishes only when $\mathbf{R}^{k\ell} = \mathbf{0}$ for $k \neq \ell$, $\ell = 1, \ldots, K$.

Here, a special case is worth considering in which $\mathbf{C}_{\mathbf{x}} = \mathrm{bdiag}(\mathbf{C}_{\mathbf{x}}^{11}, \dots, \mathbf{C}_{\mathbf{x}}^{KK})$; in other words, the mixtures (43) are uncorrelated, and there are only higher-order dependencies, if any. Then, $\mathbf{C}_{\mathbf{z}}$ joins the block-diagonal structure, so it is reasonable to select $\mathbf{R}^{k\ell} = \mathbf{0}$ for $k \neq \ell$, although the sample covariances $\hat{\mathbf{C}}_{\mathbf{z}}^{k\ell}$ are not exactly zero. In that case, (49) is simplified to

$$\frac{\partial \mathcal{J}}{\partial \mathbf{w}^{kH}} = \mathbf{a}^k - \frac{1}{N} \mathbf{X}^k \phi^k (\hat{\mathbf{s}}^1, \dots, \hat{\mathbf{s}}^K)^T.$$
 (52)

This observation is in agreement with the literature. The joint separation of correlated mixtures can be achieved using only second-order statistics [6], [51]. Uncorrelated mixtures arise, for instance, in the frequency-domain separation of convolutive mixtures. Here, the non-Gaussianity and higher-order moments are necessary for separating the mixtures [9], [52].

C. Gradient algorithms for IVE

The constrained gradient can, similarly to (52) and (39), be computed with respect to $(\mathbf{a}^k)^H$, which gives (we skip the detailed computation)

$$\frac{\partial \mathcal{J}}{\partial \mathbf{a}^{kH}} = \mathbf{w}^{k} - \frac{\lambda_{\mathbf{a}}^{k}}{N} (\widehat{\mathbf{C}}_{\mathbf{x}}^{kk})^{-1} \mathbf{X}^{k} \phi^{k} (\widehat{\mathbf{s}}^{1}, \dots, \widehat{\mathbf{s}}^{K})^{T},$$
(53)

where $\lambda_{\mathbf{a}}^k = \left(\mathbf{a}^{kH}(\widehat{\mathbf{C}}_{\mathbf{x}}^{kk})^{-1}\mathbf{a}^k\right)^{-1}$. Now, the gradient optimization algorithms for IVE (considering only sets of uncorrelated instantaneous mixtures) can proceed in the same way as those for ICE with the following differences:

- 1) In each iteration, \mathbf{w}_k or \mathbf{a}_k are updated by adding a step in the direction of the gradient (52) or (53), respectively, for each k = 1, ..., K.
- 2) The nonlinear functions ϕ^k , k = 1, ..., K, depend on the current outputs of all K iterative algorithms, which fact makes them mutually dependent.

We will refer to these algorithms as to $OGIVE_{\mathbf{w}}$ and $OGIVE_{\mathbf{a}}$, respectively; for illustration, $OGIVE_{\mathbf{w}}$ is described in Algorithm 4.

Algorithm 4: OGIVE_w: orthogonally constrained extraction of an independent vector component from the set of mutually uncorrelated mixtures $\mathbf{X}^1, \dots, \mathbf{X}^K$

```
Input: \mathbf{X}^k, \mathbf{w}_{\text{ini}}^k, k = 1, \dots, K, \mu, \text{ tol}
      Output: a^k, w^k, k = 1, ..., K
  1 foreach k = 1, \ldots, K do
            \widehat{\mathbf{C}}_{\mathbf{x}}^{kk} = \mathbf{X}^k (\mathbf{X}^k)^H / N;
              \mathbf{w}^k = \mathbf{w}_{\text{ini}}^k;
  4 end
  5 repeat
               foreach k = 1, \ldots, K do
                      \mathbf{a}^k \leftarrow ((\mathbf{w}^k)^H \widehat{\mathbf{C}}_{\mathbf{x}}^{kk} \mathbf{w}^k)^{-1} \widehat{\mathbf{C}}_{\mathbf{x}}^{kk} \mathbf{w}^k;
  7
                     \widehat{\mathbf{s}}^k \leftarrow (\mathbf{w}^k)^H \mathbf{X}^k:
  8
               end
  9
              foreach k = 1, \dots, K do
10
                      \nu^k \leftarrow \widehat{\mathbf{s}}^k \phi^k (\widehat{\mathbf{s}}^1, \dots, \widehat{\mathbf{s}}^K)^T / N;
11
                      \Delta^k \leftarrow \mathbf{a}^k - (\nu^k)^{-1} \mathbf{X}^k \phi^k (\widehat{\mathbf{s}}^1, \dots, \widehat{\mathbf{s}}^K)^T / N;
12
                      \mathbf{w}^k \leftarrow \mathbf{w}^k + \mu \Delta^k;
13
               end
14
15 until \max\{\|\Delta^1\|,\ldots,\|\Delta^K\|\} < \mathsf{tol};
```

Finally, we introduce a method referred to as $OGIVE_s$. Here, the idea presented in Section III-D is applied to the set of K mixtures. The parameter in which the gradient optimization proceeds is selected based on the heuristic criterion (42). It is important that the selection can be different for each mixture. As shown in Section III-D, the effectiveness of this optimization depends on the initial SIR, which can be different for each mixture.

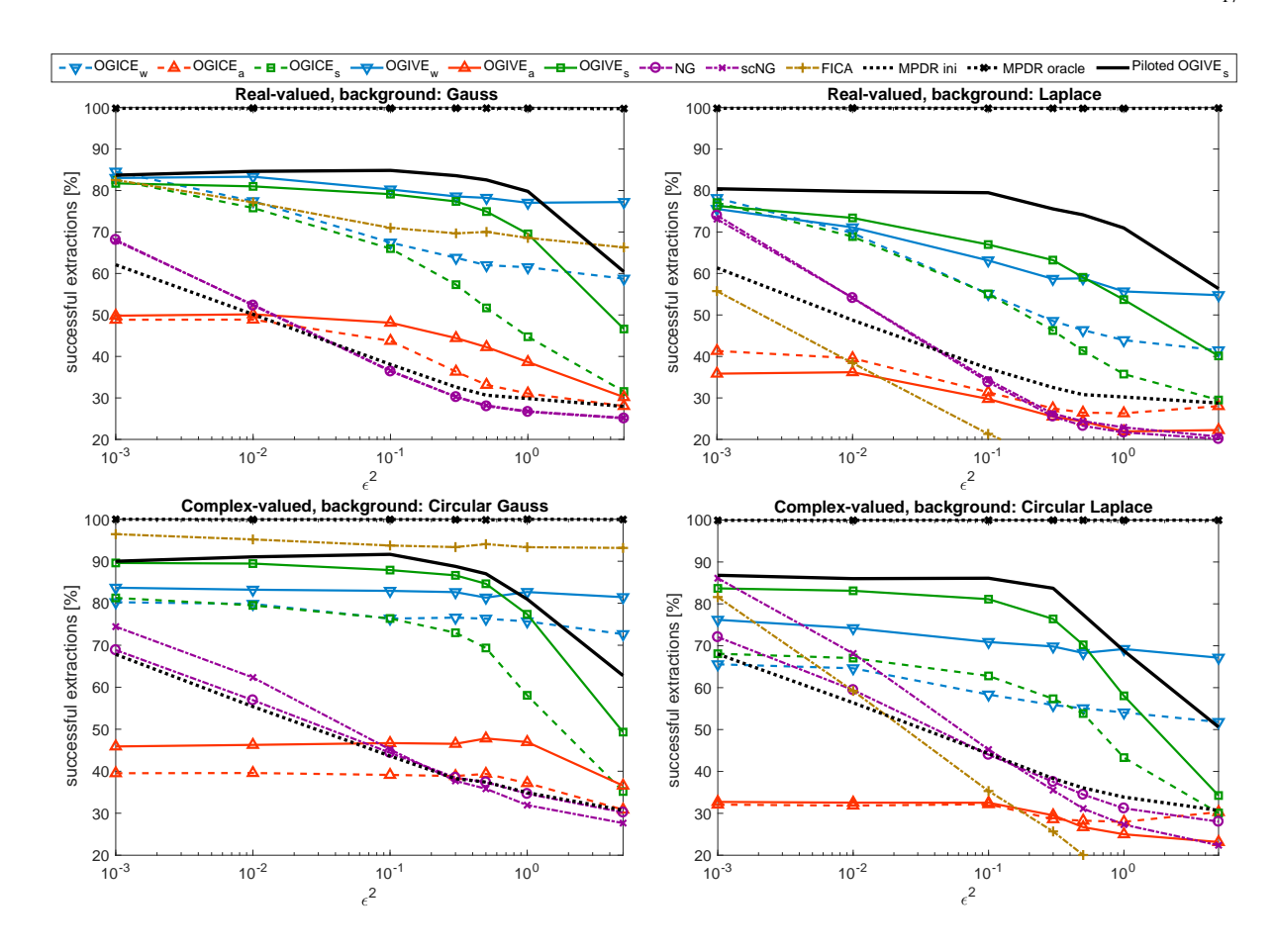


Fig. 2. Percentages of successful extractions (SIR improvement is higher than 0 dB) as functions of the initial mean squared error ϵ^2 when d=6, K=4, and N=1000. The experiment was repeated in 1000 trials (1000 \times K mixtures). The SOI is generated from Laplace components while the background is Gaussian (column 1) or Laplacean (column 2). The first row corresponds to the real-valued scenario while the second row shows results of the complex-valued case with circular variants of the signals' distributions.

V. SIMULATIONS

In simulations, we focus on the assessment of the proposed algorithms and compare them with other methods. The real-valued as well as the (circular) complex-valued versions of the experiments are considered.

In one trial, K instantaneous mixtures are generated with random mixing matrices \mathbf{A}^k , $k=1,\ldots,K$. The SOIs for these mixtures are obtained as K signals drawn independently from the Laplacean distribution and mixed by a random unitary matrix; hence, they are uncorrelated and dependent. The background is obtained by generating independent components u_2^k,\ldots,u_d^k from the Gaussian or Laplacean distribution, $k=1,\ldots,K$.

For each mixture, the SIR_{in} defined by (40) is selected uniformly at random in the range of -20 to 20 dB. The mixing matrices are drawn from the uniform distribution on interval [1;2]; or the real part in [1;2] and the imaginary part in [0,1] in the complex-valued case. This choice helps us keep the initial SIR approximately equal to SIR_{in} across all channels.

The comparison involves One-Unit FastICA (FICA) [26], three variants of OGICE proposed in Section III, the Natural Gradient algorithm (NG) [48] and its scaled version (scNG) [50], as well as three variants of OGIVE proposed in Section IV-C. These algorithms are initialized by $\mathbf{a}_{\rm ini} = \mathbf{a} + \mathbf{e}_{\rm ini}$, where \mathbf{a} is the true mixing vector,

and $e_{\rm ini}$ is a random vector with Gaussian entries such that $\|e_{\rm ini}\|^2 = \epsilon^2$. The algorithms NG and scNG are initialized by the de-mixing matrix whose first row is equal to (22) where $\mathbf{a} = \mathbf{a}_{\rm ini}$; the other rows are selected as in (8), which means that the initial background subspace is orthogonal to the initial SOI estimate.

Next, we also evaluate the SOI estimates obtained through (22) for a equal to the true mixing vector (MPDR oracle) and for $\mathbf{a} = \mathbf{a}_{\rm ini}$ (MPDR ini). While the performance of the MPDR oracle gives an upper bound, that of MPDR ini corresponds to a "do-nothing" solution purely relying on the initialization. An improvement is achieved by a blind algorithm when its performance is higher than that of MPDR ini.

ICE/ICA methods are applied to each mixture separately, while IVE algorithms treat all K mixtures jointly. The nonlinearity $\phi(\xi) = \overline{\tanh}(\xi)$ is selected in the variants of OGICE and NG. FICA is used with $\tanh(\xi)$ in the real-valued cases, or with $(1+|\xi|^2)^{-1}$ in the complex-valued simulations [53]. For IVE algorithms, the choice is

$$\phi^k(\xi^1, \dots, \xi^K) = \overline{\tanh}(\xi^k) / \sqrt{\sum_{\ell=1}^K |\xi^\ell|^2}.$$
 (54)

The problem of choosing an appropriate nonlinearity for the given method would go beyond the scope of this paper; see, e.g., [29], [44], [54].

For the sake of completeness, we also include a semi-blind variant of OGIVE_s, which is modified in a way similar to that proposed in [55]. Specifically, a "pilot" component p is assumed to be available such that the SOIs within the K mixtures are dependent on it (usually there are only higher-order dependencies; see [9]). OGIVE_s is modified only by adding the K + 1th variable into (54), which is $\xi_{K+1} = p$. In simulations, p is a random mixture of the SOIs. This method will be referred to as "Piloted OGIVE_s".

The ICA/ICE and IVE algorithms are halted when the number of iterations exceeds 1000 and $K \times 1000$, respectively. The stopping criterion is tol = 10^{-2} in the case of the proposed ICE/IVE methods, 10^{-3} for NG and scNG, and 10^{-6} for FICA. The step length μ was set to 0.1 for the proposed algorithms, and 0.02 for NG and scNG; these values were selected to ensure the stability and good performance of the methods.

A. Successful extractions

Naturally, none of the given blind algorithms extract the SOI in every trial. This mostly depends on the initialization but also on other parameters of the experiment and on the algorithm itself.

The blind extraction is assessed by the SIR improvement, that is, by the ratio between SIR_{ini} and the SIR of the extracted source. The extraction is classed as *successful* if the SIR improvement is greater than 0 dB.

In the first experiment, we focus on the percentage of successful extractions as it depends of the initial error $\|\mathbf{e}_{\text{ini}}\|^2 = \epsilon^2$. The algorithms were tested in 1000 trials for d=6, K=4, and N=1000. Fig. 2 shows the resulting percentage (out of $1000 \times K$ mixtures) achieved by the compared methods in four scenarios. MPDR oracle achieves 100% up to very few cases, which means that the ISR improvement is possible in almost all trials. The percentage by MPDR ini is decaying with growing ϵ^2 . We summarize the other important facts about our results as follows.

1) NG and scNG: These popular ICA algorithms do not improve much as compared to MPDR ini unless $\epsilon^2 \le 10^{-2}$, which points to their sensitivity to the initialization. Since these methods estimate all components

in the mixture, it happens in many cases that the SOI is extracted in a different output channel than in the desired one. $OGICE_{\mathbf{w}}$ and $OGICE_{\mathbf{s}}$ and their IVE variants show significantly better behavior in this respect.

- 2) FICA shows excellent results when the background is Gaussian. Since it is a fixed-point algorithm, it has good ability to avoid shallow extremes of the contrast function that correspond to Gaussian components. Therefore, its global convergence is very good when there are no other non-Gaussian components than the SOI. For the same reason, FICA yields pure success rate when the background is Laplacean, since it often extracts other than the desired non-Gaussian component.
- 3) **Optimization in a/w:** OGICE_a yields a significantly lower success rate than OGICE_w. Fig. 3 provides a deeper insight where the evaluation is done separately for cases when $SIR_{in} > -10$ dB and $SIR_{in} < -10$ dB, respectively. The latter case embodies mixtures where the SOI is weaker than the background, which is, according to Section III-D, preferable for the optimization in a. Here, OGICE_a outperforms OGICE_w. By contrast, OGICE_w is significantly better for $SIR_{in} > -10$ dB, which involves approximately 75% of mixtures. In conclusion, the optimization in a is less stable and is exploitable only when SIR_{in} is sufficiently low.
- 4) OGICE_s: The switched optimization gives a success rate improved by up to 10% compared to OGICE_w, but only when $\epsilon^2 < 0.5$. For higher ϵ^2 , that is, when the initial mixing vector is more distant from the true value, OGICE_w performs better. The detailed results shown in Fig. 3 indicate that OGICE_s is worse compared to OGICE_w when SIR_{in} > -10 dB and $\epsilon^2 \ge 0.5$. In these cases, the criterion (42) suggests selecting the optimization in a, which impairs the success rate of OGICE_s. To avoid this drawback, a better decision rule (prediction of SIR_{in}) is needed, which we leave for future research.
- 5) ICE vs IVE: The IVE variants of the proposed algorithms mostly achieve better results than their ICE counterparts. They take advantage of the dependencies between SOIs in different mixtures, which helps to extend the region of convergence, thereby improving the success rate. The comparison of OGIVE_a, OGIVE_w and OGIVE_s leads to conclusions similar to their ICE counterparts.
- 6) **Piloted OGIVE**_s: Finally, this algorithm achieves superior results as it exploits the dependent component to keep converging to the SOI. Its performance is reduced when $\epsilon^2 \geq 0.5$ due to the shortage of the criterion (42), as mentioned in Item 4 above.

Fig. 4 shows results of the experiment for a fixed value $\epsilon^2 = 0.1$ when d is varied from 2 through 20. Here, the compared methods confirm their behavior observed in the previous example. While the performance of FICA, NG, scNG, OGICE_a and OGIVE_a is decaying with growing dimension d, the other OGICE and OGIVE variants yield results which are significantly more stable.

OGICE_s and OGIVE_s outperform OGICE_w and OGIVE_w, respectively, mostly when $d \leq 10$. We verified in other simulations that, for higher dimensions, the performance can be improved by setting higher τ so that switching to the optimization in a in OGICE_s or OGIVE_s is more selective.

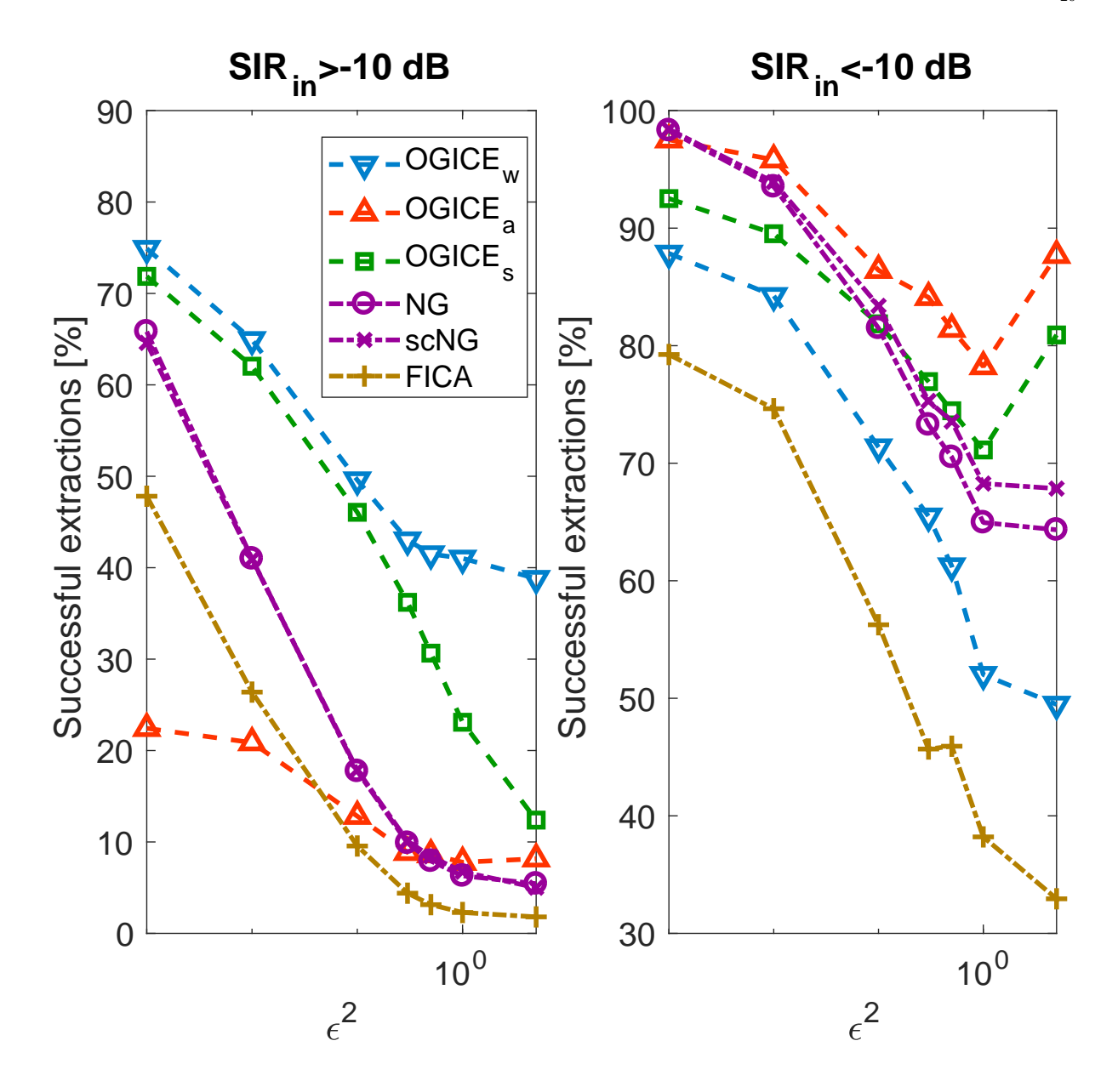


Fig. 3. Percentage of successful extractions for the real-valued scenario with Laplacean background evaluated separately for mixtures where $SIR_{in} > -10$ dB and $SIR_{in} < -10$ dB, respectively. In this comparison, IVA algorithms cannot be included, because they are applied to K=4 mixtures jointly where $SIR_{in} \in [-20,20]$ dB.

B. Signal-to-Interference Ratio

The empirical distributions of SIR measurements from the trials of the previous experiments are heavy-tailed. Each algorithm extracts the correct source in different percentages of trials as shown by the previous results, so it is hard to compare their performances in terms of SIR.

Figures 5 and 6 show median SIR improvement as functions of ϵ^2 and d, respectively. The complex-valued cases are shown here when the background is Gaussian or Laplacean.

 $OGICE_a$ and $OGIVE_a$ yield results below 0 dB up to situations when d < 6. This is caused by the fact that their success rate is lower than 50% for the other values of the parameters. NG, and similarly NGsc, also get

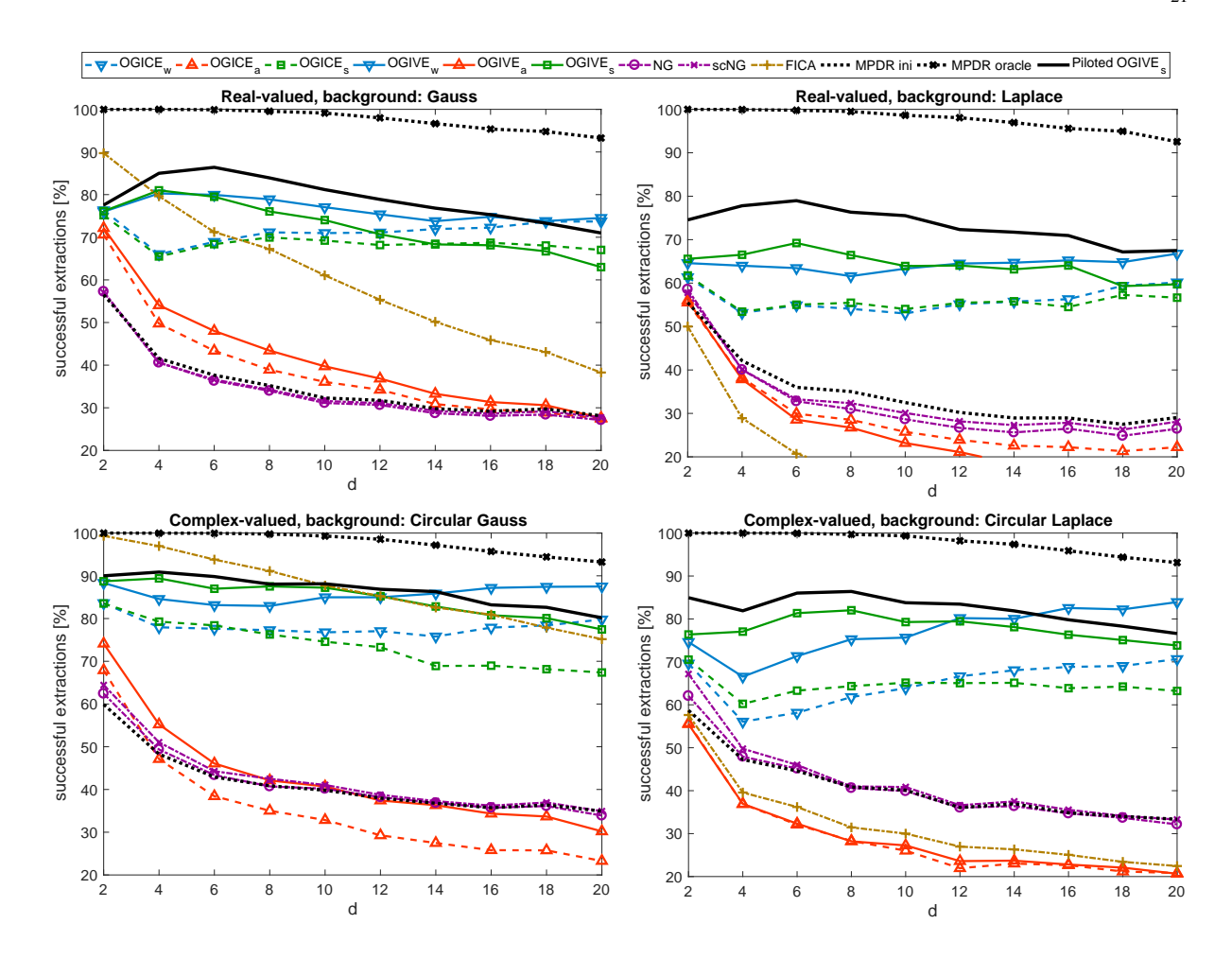


Fig. 4. Percentages of successful extractions achieved in 1000 trials with random SIR_{in} for a varying number of source d from 2 through 20 when $\epsilon^2 = 0.1$, K = 4, and N = 1000.

below 0 dB for d > 6; however, Fig. 5 indicates that these algorithms can achieve a good median SIR when initialized within a very close vicinity of the correct solution.

In Fig. 5, FICA confirms its excellent global convergence when the background is Gaussian; however, it is highly sensitive to the initialization when the background is non-Gaussian.

Stable median SIR is achieved by the other proposed ICE and IVE methods, where the best results are achieved by Piloted OGIVE_s, OGIVE_w and OGIVE_s. Fig. 5 shows that the latter method fails when $\epsilon^2 > 1$.

C. Computational Aspects

Fig. 7 shows average computational time needed by the algorithms to process one mixture in the experiment where d is varied. The results are divided into the cases where $\mathrm{SIR_{in}} > -10~\mathrm{dB}$ and $\mathrm{SIR_{in}} < -10~\mathrm{dB}$. NG, NGsc and FICA behave similarly in both cases. FICA is very fast as it requires few (say, fewer than 20) iterations to meet the stopping condition. NG and NGsc are slow compared to the other methods as they separate the whole mixture. A deeper inspection, however, also showed that they need a considerably higher number of iterations to converge than the ICE/IVE methods.

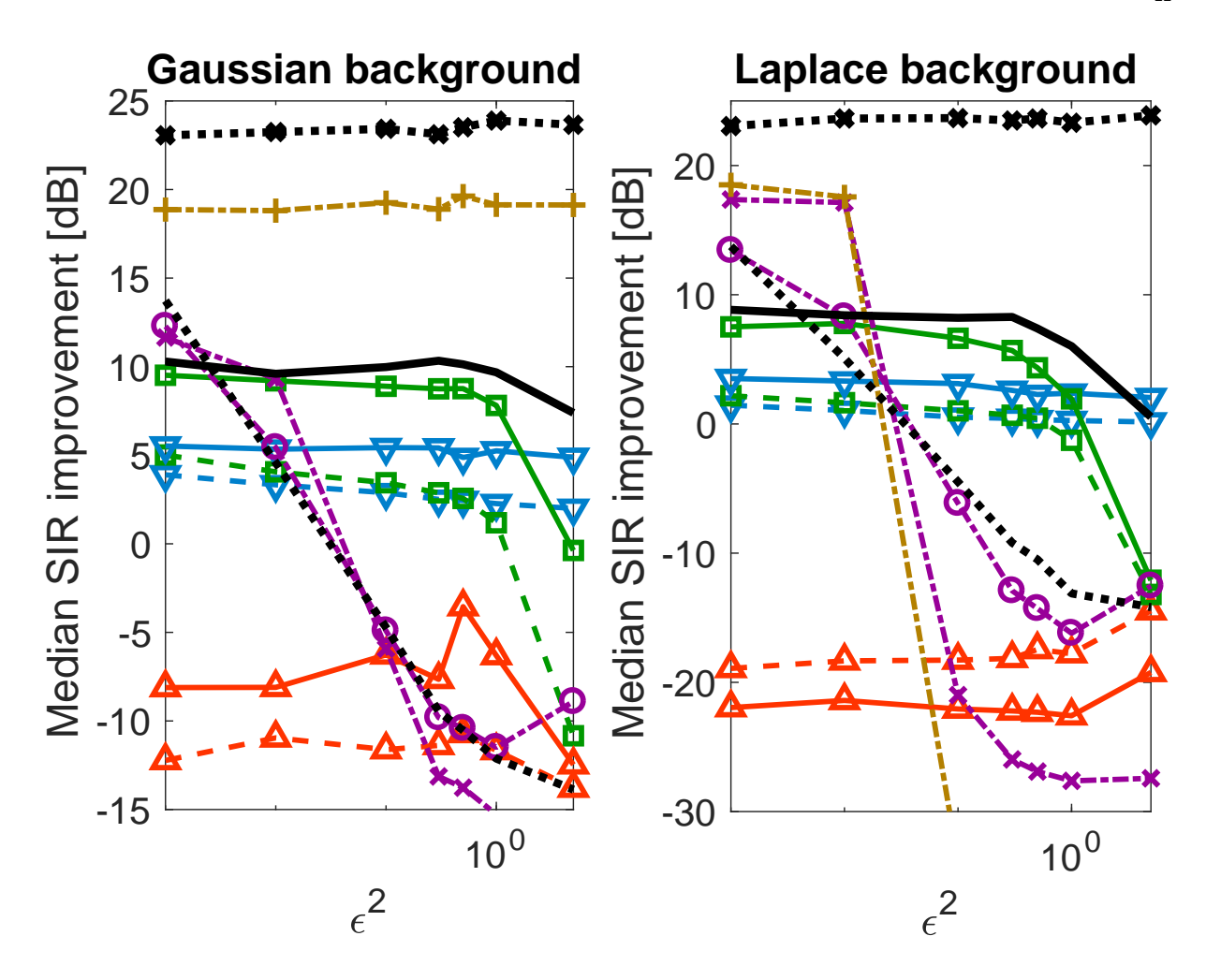


Fig. 5. Median SIR improvement as function of the initial mean squared error ϵ^2 ; the complex-valued data. Legend for this figure is the same as that of Fig. 4.

OGICE_a is significantly faster than OGICE_w when $SIR_{in} < -10$ dB, while the latter is slightly faster (since d > 8) when $SIR_{in} > -10$ dB. The computational time of OGICE_s is between those of the two variants, which points to the effectiveness of the switching optimization.

The variants of OGIVE need similar computational times for $SIR_{in} > -10$ dB as well as for $SIR_{in} < -10$ dB; to a certain extent, they copy the behavior of their OGICE counterparts, but are significantly slower. This is caused by the fact that K mixtures are processed simultaneously, so the computational time is averaged over four mixtures from each trial (with both high andlow SIR_{in}).

VI. CONCLUSIONS

We have revised the problem of blind source extraction of an independent target source from background signals and introduced the concept of Independent Component Extraction. Based on the maximum likelihood principle, several variants of gradient algorithms have been derived, also for the joint extraction of vector components from a set of mixtures. The simulation study has compared these methods with popular NG, NGsc and FICA. The proposed methods of optimizing the separating vector show a much higher stability of

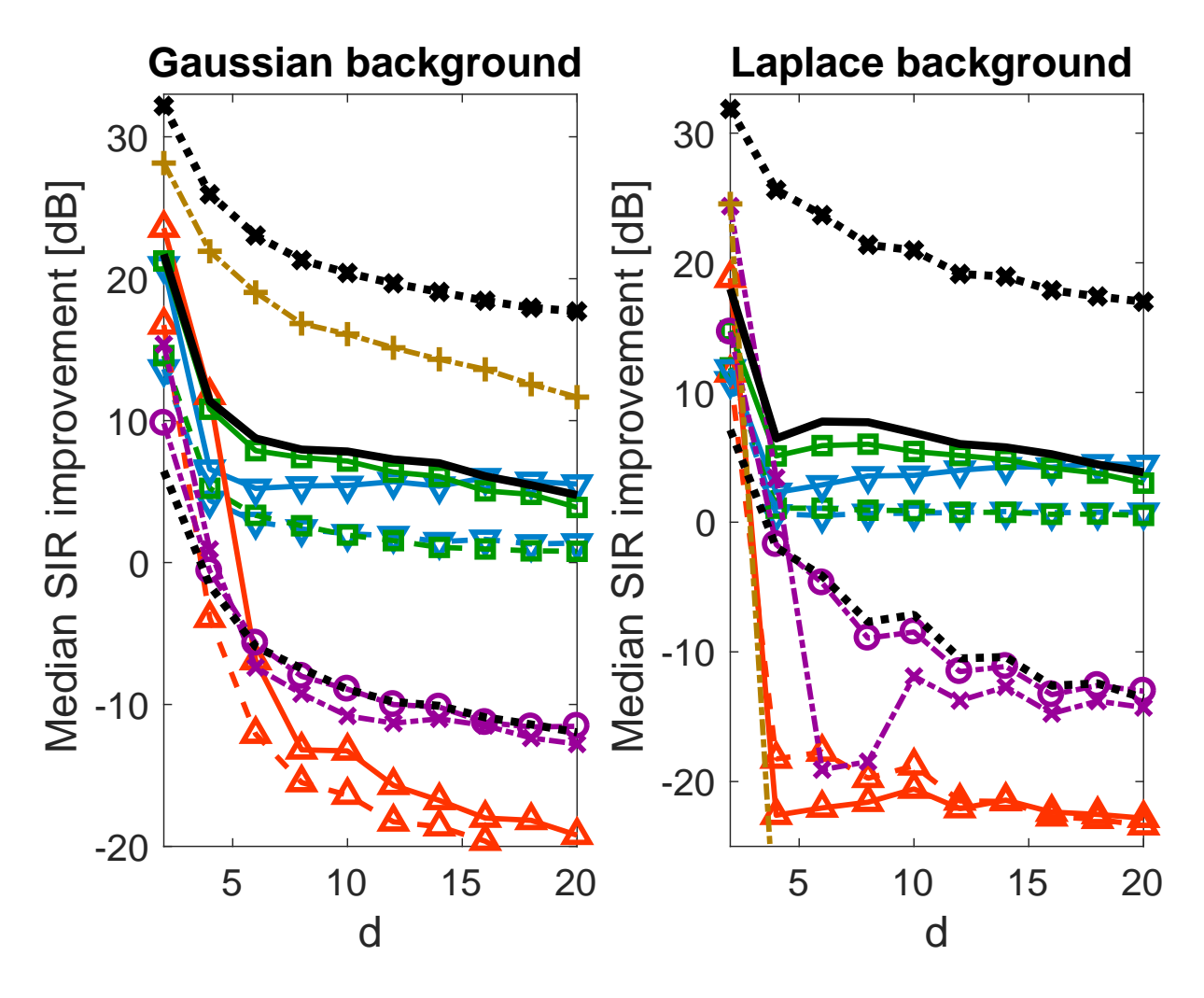


Fig. 6. Median SIR improvement as function of the dimension d; the complex-valued data. Legend for this figure is the same as that of Fig. 4.

convergence (OGICE $_{\mathbf{w}}$, OGIVE $_{\mathbf{w}}$) than NG and NGsc for a wide variety of SIR $_{\mathrm{in}}$, while those optimizing the mixing vector (OGICE $_{\mathbf{a}}$, OGIVE $_{\mathbf{a}}$) are stable only when SIR $_{\mathrm{in}}<-10$ dB. We have also shown that a switched optimization can take advantage of the two approaches and improve stability and convergence speed (OGICE $_{\mathbf{s}}$, OGIVE $_{\mathbf{s}}$) provided that SIR $_{\mathrm{in}}$ is correctly predicted.

The results have also revealed room for further improvements. Gradient algorithms are considerably slower compared to, e.g., FICA. The speed could be improved using, e.g., a Newton-like optimization scheme; however, faster convergence must not be paid for by decreased stability. The Another aspect is the accuracy. Future methods should be capable of avoiding spurious local minima in the vicinity of the desired solution. From a theoretical point of view, ICE/IVE algorithms can improve their overall properties when they are capable of exploiting the non-Gaussianity/nonstationarity/non-whiteness of the background.

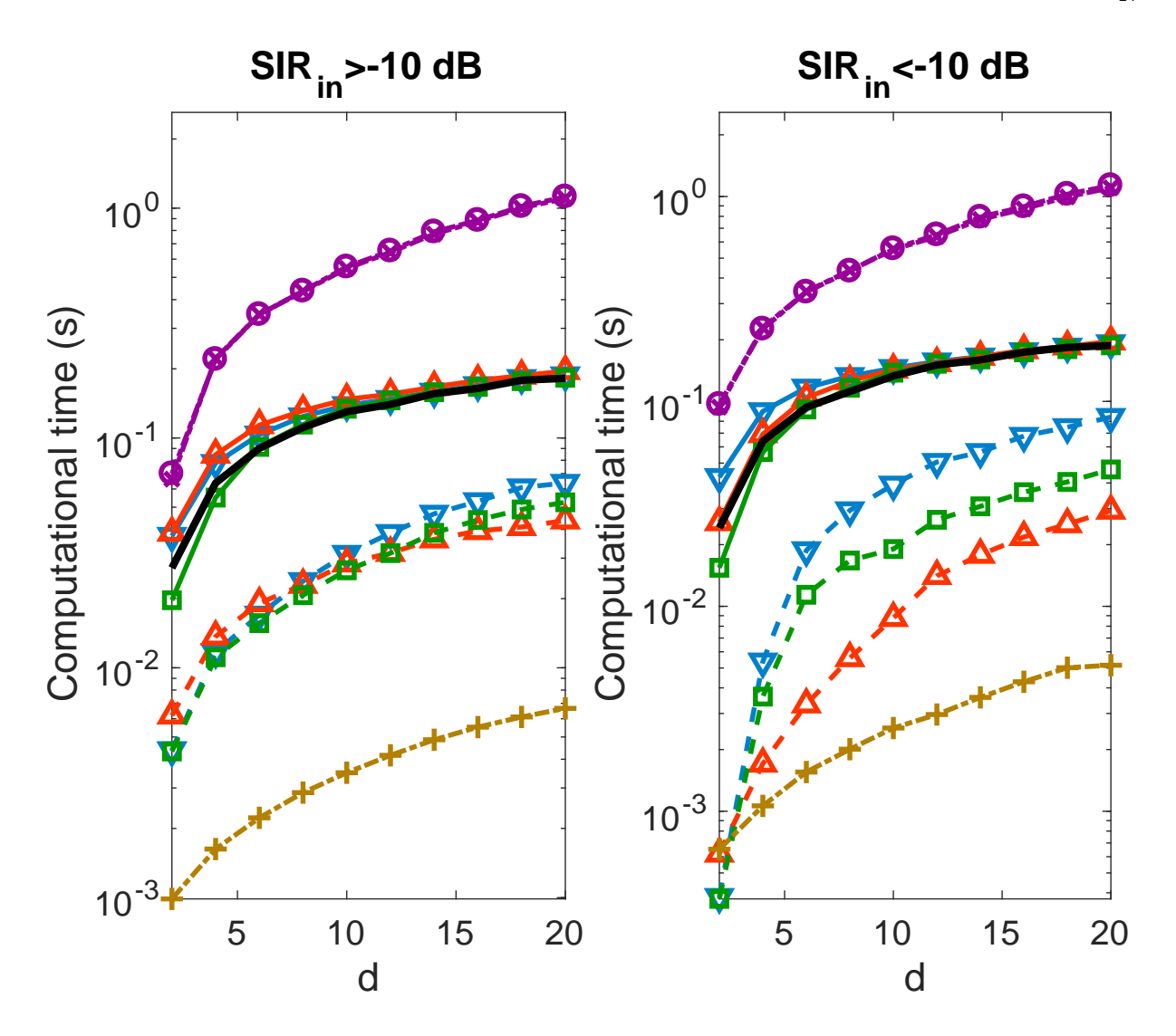


Fig. 7. Computational time as function of the number of signals d evaluated on a PC with two Intel Xeon processors, 12 cores 2.6 GHz, using Matlab R2017b with Parallel Computing Toolbox; real-valued data; Gaussian background. Legend for this figure is the same as that of Fig. 4.

APPENDIX A: PROOF OF (22) AND (23)

Since y = Qz = QBx, we can introduce the projection operator $\Pi_y = QB$, which is equal to

$$\mathbf{\Pi}_{\mathbf{y}} = \mathbf{I}_d - \mathbf{a}\mathbf{w}^H. \tag{55}$$

According to (21), the OC can be written as

$$\widehat{\mathbf{Z}}^H \widehat{\mathbf{s}}/N = \mathbf{B}\widehat{\mathbf{C}}_{\mathbf{x}} \mathbf{w} = \mathbf{0}. \tag{56}$$

By multiplying the latter equation from the left by Q and using (55), we arrive at

$$(\mathbf{I}_d - \mathbf{a}\mathbf{w}^H)\widehat{\mathbf{C}}_{\mathbf{x}}\mathbf{w} = \mathbf{0},\tag{57}$$

$$\mathbf{w} - \widehat{\mathbf{C}}_{\mathbf{x}}^{-1} \mathbf{a} \left(\mathbf{w}^{H} \widehat{\mathbf{C}}_{\mathbf{x}} \mathbf{w} \right) = \mathbf{0}.$$
 (58)

By multiplying (58) from the left by \mathbf{a}^H it follows

$$\mathbf{a}^H \mathbf{w} - \mathbf{a}^H \widehat{\mathbf{C}}_{\mathbf{x}}^{-1} \mathbf{a} \, \mathbf{w}^H \widehat{\mathbf{C}}_{\mathbf{x}} \mathbf{w} = \mathbf{0}, \tag{59}$$

and since $\mathbf{a}^H \mathbf{w} = 1$, it holds that

$$\mathbf{a}^H \hat{\mathbf{C}}_{\mathbf{x}}^{-1} \mathbf{a} = (\mathbf{w}^H \hat{\mathbf{C}}_{\mathbf{x}} \mathbf{w})^{-1}. \tag{60}$$

By putting (58) and (60) together, (22) and (23) follow.

APPENDIX B: PROOF OF (25)

Assume that \mathbf{a} is equal to its true value in (2) (hence $\mathbf{A} = \mathbf{A}_{\rm ICE}$ and $\mathbf{W} = \mathbf{W}_{\rm ICE}$), and recall that, in the determined ICE model, $\mathbf{y} = \mathbf{Q}\mathbf{z}$ holds. Then, $\mathbf{w}_{\rm MPDR}^H\mathbf{x} = s + \mathbf{w}_{\rm MPDR}^H\mathbf{y}$. We should show that $\mathbf{a}^H\mathbf{C}_{\mathbf{x}}^{-1}\mathbf{y} = \mathbf{0}$. It holds that

$$\mathbf{a}^{H}\mathbf{C}_{\mathbf{x}}^{-1}\mathbf{y} = \mathbf{a}^{H}\mathbf{C}_{\mathbf{x}}^{-1}\mathbf{Q}\mathbf{z} \tag{61}$$

$$= \mathbf{a}^H \left(\mathbf{A} \mathbf{C}_{\mathbf{v}} \mathbf{A}^H \right)^{-1} \mathbf{Q} \mathbf{z} \tag{62}$$

$$= \mathbf{a}^H \mathbf{W}^H \mathbf{C}_{\mathbf{v}}^{-1} \mathbf{W} \mathbf{Q} \mathbf{z}, \tag{63}$$

where $\mathbf{C_v} = \mathrm{E}[\mathbf{v}\mathbf{v}^H]$. Next, it holds that $\mathbf{a}^H\mathbf{W}^H = [1, \mathbf{0}^H]$, and $\mathbf{W}\mathbf{Q} = [\mathbf{0}, \mathbf{I}_{d-1}]^H$. By taking into account the block-diagonal structure of $\mathbf{C_v}$, i.e.,

$$\mathbf{C_v} = \begin{pmatrix} \sigma_s^2 & \mathbf{0}^H \\ \mathbf{0} & \mathbf{C_z} \end{pmatrix},\tag{64}$$

where σ_s^2 denotes the variance of s, (25) follows.

APPENDIX C: COMPUTATION OF (27)

The following identities hold under the constraint (23).

$$\mathbf{g} = \mathbf{E} \,\mathbf{a} = \frac{\mathbf{E} \hat{\mathbf{C}}_{\mathbf{x}} \mathbf{w}}{\mathbf{w}^H \hat{\mathbf{C}}_{\mathbf{x}} \mathbf{w}},\tag{65}$$

$$\gamma = \mathbf{e}_1^H \mathbf{a} = \frac{\mathbf{e}_1^H \hat{\mathbf{C}}_{\mathbf{x}} \mathbf{w}}{\mathbf{w}^H \hat{\mathbf{C}}_{\mathbf{x}} \mathbf{w}},\tag{66}$$

$$1 - \mathbf{h}^{H} \mathbf{g} = \overline{\beta} \gamma = \overline{\beta} \frac{\mathbf{e}_{1}^{H} \widehat{\mathbf{C}}_{\mathbf{x}} \mathbf{w}}{\mathbf{w}^{H} \widehat{\mathbf{C}}_{\mathbf{x}} \mathbf{w}}.$$
(67)

To derive (27), we proceed by computing the derivatives of the three terms in (26). First, using (28), it follows that

$$\frac{\partial}{\partial \mathbf{w}^H} \log f(\mathbf{w}^H \mathbf{x}) = -\phi(\mathbf{w}^H \mathbf{x}) \mathbf{x}, \tag{68}$$

so that

$$\frac{1}{N} \sum_{n=1}^{N} -\phi(\mathbf{w}^H \mathbf{x}(n)) \mathbf{x}(n) = -\frac{1}{N} \mathbf{X} \phi(\mathbf{w}^H \mathbf{X})^T,$$
(69)

where $\phi(\cdot)$ is applied element-wise in case of the vector argument.

Let \mathbf{x} be partitioned as $\mathbf{x} = [x_1; \mathbf{x}_2]$. Under the constraint (23) and using $\mathbf{B} = [\mathbf{g}, -\gamma \mathbf{I}_{d-1}]$, the second term in (26) (where the argument n is omitted) can be re-written as

$$\mathbf{x}^{H}\mathbf{B}^{H}\mathbf{R}\mathbf{B}\mathbf{x} = (\mathbf{w}^{H}\widehat{\mathbf{C}}_{\mathbf{x}}\mathbf{w})^{-1} \times$$

$$(|x_{1}|^{2}\mathbf{w}^{H}\widehat{\mathbf{C}}_{\mathbf{x}}\mathbf{E}^{H}\mathbf{R}\mathbf{E}\widehat{\mathbf{C}}_{\mathbf{x}}\mathbf{w} - \overline{x_{1}}\mathbf{w}^{H}\widehat{\mathbf{C}}_{\mathbf{x}}\mathbf{E}^{H}\mathbf{e}_{1}^{H}\widehat{\mathbf{C}}_{\mathbf{x}}\mathbf{w}\mathbf{R}\mathbf{x}_{2} -$$

$$x_{1}\mathbf{w}^{H}\widehat{\mathbf{C}}_{\mathbf{x}}\mathbf{e}_{1}\mathbf{x}_{2}^{H}\mathbf{R}\mathbf{E}\widehat{\mathbf{C}}_{\mathbf{x}}\mathbf{w} + \mathbf{w}^{H}\widehat{\mathbf{C}}_{\mathbf{x}}\mathbf{e}_{1}\mathbf{x}_{2}^{H}\mathbf{R}\mathbf{e}_{1}^{H}\widehat{\mathbf{C}}_{\mathbf{x}}\mathbf{w}\mathbf{x}_{2}). \quad (70)$$

By taking the derivative under the OG and after some rearrangements,

$$\frac{\partial}{\partial \mathbf{w}^{H}} \mathbf{x}^{H} \mathbf{B}^{H} \mathbf{R} \mathbf{B} \mathbf{x} = -2\mathbf{a} \, \mathbf{x}^{H} \mathbf{B}^{H} \mathbf{R} \mathbf{B} \mathbf{x} + (\mathbf{w}^{H} \widehat{\mathbf{C}}_{\mathbf{x}} \mathbf{w})^{-1} \times (\overline{\mathbf{x}_{1}} \widehat{\mathbf{C}}_{\mathbf{x}} \mathbf{E}^{H} \mathbf{R} \mathbf{B} \mathbf{x} - \mathbf{x}_{2}^{H} \mathbf{R} \mathbf{B} \mathbf{x} \widehat{\mathbf{C}}_{\mathbf{x}} \mathbf{e}_{1}). \quad (71)$$

By considering the averages of the above terms over N samples, we arrive at the following chain of identities:

$$\frac{1}{N} \sum_{n=1}^{N} \mathbf{x}(n)^{H} \mathbf{B}^{H} \mathbf{R} \mathbf{B} \mathbf{x}(n) = \frac{1}{N} \sum_{n=1}^{N} \operatorname{tr}(\mathbf{B}^{H} \mathbf{R} \mathbf{B} \mathbf{x}(n)^{H} \mathbf{x}(n))$$

$$= \operatorname{tr}(\mathbf{R} \mathbf{B} \hat{\mathbf{C}}_{\mathbf{x}} \mathbf{B}^{H}) = \operatorname{tr}(\mathbf{R} \hat{\mathbf{C}}_{\mathbf{z}}). \tag{72}$$

Next,

$$\frac{1}{N} \sum_{n=1}^{N} \overline{x_{1}}(n) \widehat{\mathbf{C}}_{\mathbf{x}} \mathbf{E}^{H} \mathbf{R} \mathbf{B} \mathbf{x}(n) = \widehat{\mathbf{C}}_{\mathbf{x}} \mathbf{E}^{H} \mathbf{R} \mathbf{B} \mathbf{X} \mathbf{X}^{H} \mathbf{e}_{1} / N$$

$$= \widehat{\mathbf{C}}_{\mathbf{x}} \mathbf{E}^{H} \mathbf{R} \widehat{\mathbf{Z}} \mathbf{X}^{H} \mathbf{e}_{1} / N$$

$$= \widehat{\mathbf{C}}_{\mathbf{x}} \mathbf{E}^{H} \mathbf{R} \widehat{\mathbf{C}} \left(\widehat{\mathbf{s}}^{H} \quad \widehat{\mathbf{Z}}^{H} \right) \mathbf{A}_{\text{ICE}}^{H} \mathbf{e}_{1} / N$$

$$= \widehat{\mathbf{C}}_{\mathbf{x}} \mathbf{E}^{H} \mathbf{R} \left(\mathbf{0}^{H} \quad \widehat{\mathbf{C}}_{\mathbf{z}} \right) \mathbf{A}_{\text{ICE}}^{H} \mathbf{e}_{1}$$

$$= \widehat{\mathbf{C}}_{\mathbf{x}} \mathbf{E}^{H} \mathbf{R} \widehat{\mathbf{C}}_{\mathbf{z}} \mathbf{h}, \tag{73}$$

where we used (20) and (21). The last identity is

$$\frac{1}{N} \sum_{n=1}^{N} \mathbf{x}_{2}^{H} \mathbf{R} \mathbf{B} \mathbf{x} \hat{\mathbf{C}}_{\mathbf{x}} \mathbf{e}_{1} = \text{tr} \left(\mathbf{R} \mathbf{B} \hat{\mathbf{C}}_{\mathbf{x}} \mathbf{E}^{H} \right) \hat{\mathbf{C}}_{\mathbf{x}} \mathbf{e}_{1}. \tag{74}$$

The derivative of the third term in (26) reads

$$(d-2)\frac{\partial}{\partial \mathbf{w}^{H}}\log|\gamma|^{2} =$$

$$(d-2)\frac{\partial}{\partial \mathbf{w}^{H}}(\log|\mathbf{w}^{H}\widehat{\mathbf{C}}_{\mathbf{x}}\mathbf{e}_{1}|^{2} - \log|\mathbf{w}^{H}\widehat{\mathbf{C}}_{\mathbf{x}}\mathbf{w}|^{2}) =$$

$$(d-2)\frac{\partial}{\partial \mathbf{w}^{H}}(\log\mathbf{w}^{H}\widehat{\mathbf{C}}_{\mathbf{x}}\mathbf{e}_{1} - 2\log\mathbf{w}^{H}\widehat{\mathbf{C}}_{\mathbf{x}}\mathbf{w}) =$$

$$(d-2)\left(\frac{\widehat{\mathbf{C}}_{\mathbf{x}}\mathbf{e}_{1}}{\mathbf{w}^{H}\widehat{\mathbf{C}}_{\mathbf{x}}\mathbf{e}_{1}} - 2\frac{\widehat{\mathbf{C}}_{\mathbf{x}}\mathbf{w}}{\mathbf{w}^{H}\widehat{\mathbf{C}}_{\mathbf{x}}\mathbf{w}}\right) =$$

$$(d-2)\left(\overline{\gamma}^{-1}\frac{\widehat{\mathbf{C}}_{\mathbf{x}}\mathbf{e}_{1}}{\mathbf{w}^{H}\widehat{\mathbf{C}}_{\mathbf{x}}\mathbf{w}} - 2\mathbf{a}\right). \quad (75)$$

Now, (27) is obtained by putting together (69), (71), and (75) using the identities (72), (73), and (74).

REFERENCES

- [1] T.-W. Lee, Independent Component Analysis Theory and Applications. Kluwer Academic Publishers, 1998.
- [2] A. Hyvärinen, J. Karhunen, and E. Oja, Independent Component Analysis. John Wiley & Sons, 2001.
- [3] A. Cichocki and S. Amari, Adaptive Blind Signal and Image Processing. John Wiley & Sons, 2002.
- [4] P. Comon and C. Jutten, *Handbook of Blind Source Separation: Independent Component Analysis and Applications*, ser. Independent Component Analysis and Applications Series. Elsevier Science, 2010.
- [5] P. Smaragdis, "Blind separation of convolved mixtures in the frequency domain," Neurocomputing, vol. 22, pp. 21-34, 1998.
- [6] Y. O. Li, T. Adalı, W. Wang, and V. D. Calhoun, "Joint blind source separation by multiset canonical correlation analysis," *IEEE Transactions on Signal Processing*, vol. 57, no. 10, pp. 3918–3929, Oct 2009.
- [7] D. Lahat and C. Jutten, "Joint blind source separation of multidimensional components: Model and algorithm," in 2014 22nd European Signal Processing Conference (EUSIPCO), Sept 2014, pp. 1417–1421.
- [8] X.-L. Li, T. Adalı, and M. Anderson, "Joint blind source separation by generalized joint diagonalization of cumulant matrices," *Signal Processing*, vol. 91, no. 10, pp. 2314 2322, 2011.
- [9] T. Kim, H. T. Attias, S.-Y. Lee, and T.-W. Lee, "Blind source separation exploiting higher-order frequency dependencies," *IEEE Transactions on Audio, Speech, and Language Processing*, pp. 70–79, Jan. 2007.
- [10] H. Sawada, R. Mukai, S. Araki, and S. Makino, "Solving the permutation and the circularity problem of frequency-domain blind source separation," in *Proc. of the 18th International Congress on Acoustics (ICA 2004)*, Apr. 2004, pp. I–89–I–92.
- [11] Z. Koldovský, J. Málek, P. Tichavský, and F. Nesta, "Semi-blind noise extraction using partially known position of the target source," *IEEE Transactions on Audio, Speech, and Language Processing*, vol. 21, no. 10, pp. 2029–2041, Oct 2013.
- [12] H. Sawada, S. Araki, R. Mukai, and S. Makino, "Blind extraction of a dominant source signal from mixtures of many sources," in *Proceedings of IEEE International Conference on Audio, Speech and Signal Processing*, vol. III, Mar. 2005, pp. 61–64.
- [13] S. Javidi, D. P. Mandic, and A. Cichocki, "Complex blind source extraction from noisy mixtures using second-order statistics," *IEEE Transactions on Circuits and Systems I: Regular Papers*, vol. 57, no. 7, pp. 1404–1416, July 2010.
- [14] H. Sawada, S. Araki, R. Mukai, and S. Makino, "Blind extraction of dominant target sources using ICA and time-frequency masking," *IEEE Transactions on Audio, Speech, and Language Processing*, vol. 14, no. 6, pp. 2165–2173, Nov 2006.
- [15] S. Amari and A. Cichocki, "Adaptive blind signal processing-neural network approaches," *Proceedings of the IEEE*, vol. 86, no. 10, pp. 2026–2048, Oct 1998.
- [16] S. A. Cruces-Alvarez, A. Cichocki, and S. Amari, "From blind signal extraction to blind instantaneous signal separation: criteria, algorithms, and stability," *IEEE Transactions on Neural Networks*, vol. 15, no. 4, pp. 859–873, July 2004.
- [17] P. J. Huber, "Projection pursuit," Ann. Statist., vol. 13, no. 2, pp. 435-475, June 1985.
- [18] M. Girolami, "Extraction of independent signal sources using a deflationary exploratory projection pursuit network with lateral inhibition," *IEE Proceedings Vision, Image and Signal Processing*, vol. 144, pp. 299–306(7), October 1997.
- [19] O. Shalvi and E. Weinstein, "Super-exponential methods for blind deconvolution," *IEEE Transactions on Information Theory*, vol. 39, no. 2, pp. 504–519, Mar 1993.
- [20] J. J. Shynk and R. P. Gooch, "The constant modulus array for cochannel signal copy and direction finding," *IEEE Transactions on Signal Processing*, vol. 44, no. 3, pp. 652–660, Mar 1996.
- [21] E. Moreau and O. Macchi, "High-order contrasts for self-adaptive source separation," *International Journal of Adaptive Control and Signal Processing*, vol. 10, no. 1, pp. 19–46, 1996.
- [22] T. Cover and J. Thomas, Elements of Information Theory. Wiley, 2006.
- [23] J. F. Cardoso, "Blind signal separation: statistical principles," Proceedings of the IEEE, vol. 86, no. 10, pp. 2009–2025, Oct 1998.
- [24] N. Delfosse and P. Loubaton, "Adaptive blind separation of independent sources: A deflation approach," *Signal Processing*, vol. 45, no. 1, pp. 59 83, 1995.
- [25] A. T. Erdogan, "On the convergence of ica algorithms with symmetric orthogonalization," *IEEE Transactions on Signal Processing*, vol. 57, no. 6, pp. 2209–2221, June 2009.
- [26] A. Hyvärinen and E. Oja, "A fast fixed-point algorithm for independent component analysis," *Neural Computation*, vol. 9, no. 7, pp. 1483–1492, July 1997.
- [27] A. Hyvärinen, "Fast and robust fixed-point algorithm for independent component analysis," *IEEE Transactions on Neural Networks*, vol. 10, no. 3, pp. 626–634, 1999.

- [28] T. Wei, "A convergence and asymptotic analysis of the generalized symmetric fastica algorithm," *IEEE Transactions on Signal Processing*, vol. 63, no. 24, pp. 6445–6458, Dec 2015.
- [29] P. Tichavský, Z. Koldovský, and E. Oja, "Performance analysis of the FastICA algorithm and Cramér-Rao bounds for linear independent component analysis," *IEEE Transactions on Signal Processing*, vol. 54, no. 4, pp. 1189–1203, April 2006.
- [30] A. Hyvärinen, "One-unit contrast functions for independent component analysis: a statistical analysis," in *Neural Networks for Signal Processing VII. Proceedings of the 1997 IEEE Signal Processing Society Workshop*, Sep 1997, pp. 388–397.
- [31] J.-F. Cardoso, "On the performance of orthogonal source separation algorithms," in *Proceedings of European Signal Processing Conference*, Sep. 1994, pp. 776–779.
- [32] Z. Koldovský, P. Tichavský, and E. Oja, "Efficient variant of algorithm FastICA for independent component analysis attaining the Cramér-Rao lower bound," *IEEE Transactions on Neural Networks*, vol. 17, no. 5, pp. 1265–1277, Sept 2006.
- [33] D.-T. A. Pham, "Blind partial separation of instantaneous mixtures of sources," in *Proceedings of International Conference on Independent Component Analysis and Signal Separation*. Springer Berlin Heidelberg, 2006, pp. 868–875.
- [34] I. Lee, T. Kim, and T.-W. Lee, "Independent vector analysis for convolutive blind speech separation," in *Blind speech separation*. Springer, 2007, pp. 169–192.
- [35] T. Adalı, M. Anderson, and G. S. Fu, "Diversity in independent component and vector analyses: Identifiability, algorithms, and applications in medical imaging," *IEEE Signal Processing Magazine*, vol. 31, no. 3, pp. 18–33, May 2014.
- [36] H. L. Van Trees, Optimum Array Processing: Part IV of Detection, Estimation, and Modulation Theory. John Wiley & Sons, Inc., 2002
- [37] J. F. Cardoso, "Multidimensional independent component analysis," in *Proceedings of IEEE International Conference on Audio, Speech and Signal Processing*, vol. 4, May 1998, pp. 1941–1944 vol.4.
- [38] A. Hyvärinen and U. Köster, "FastISA: A fast fixed-point algorithm for independent subspace analysis," in 14th European symposium on artificial neural networks, (ESANN 2006), 2006.
- [39] Z. Koldovský, P. Tichavský, and V. Kautský, "Orthogonally constrained independent component extraction: Blind MPDR beamforming," in *Proceedings of European Signal Processing Conference*, Sep. 2017, pp. 1195–1199.
- [40] K. Matsuoka and S. Nakashima, "Minimal distortion principle for blind source separation," in *Proceedings of International Conference on Independent Component Analysis and Signal Separation*, Dec. 2001, pp. 722–727.
- [41] N. Duong, E. Vincent, and R. Gribonval, "Under-determined reverberant audio source separation using a full-rank spatial covariance model," *IEEE Transactions on Audio, Speech, and Language Processing*, vol. 18, no. 7, pp. 1830–1840, 2010.
- [42] Z. Koldovský and F. Nesta, "Performance analysis of source image estimators in blind source separation," *IEEE Transactions on Signal Processing*, vol. 65, no. 16, pp. 4166–4176, Aug. 2017.
- [43] H. Sawada, R. Mukai, S. Araki, and S. Makino, "A robust and precise method for solving the permutation problem of frequency-domain blind source separation," *IEEE Transactions on Speech and Audio Processing*, vol. 12, no. 5, pp. 530–538, Sep. 2004.
- [44] D. T. Pham and P. Garat, "Blind separation of mixture of independent sources through a quasi-maximum likelihood approach," *IEEE Transactions on Signal Processing*, vol. 45, no. 7, pp. 1712–1725, Jul 1997.
- [45] D. H. Brandwood, "A complex gradient operator and its application in adaptive array theory," *Communications, Radar and Signal Processing, IEE Proceedings F*, vol. 130, no. 1, pp. 11–16, February 1983.
- [46] H. Li and T. Adalı, "Complex-valued adaptive signal processing using nonlinear functions," *EURASIP Journal on Advances in Signal Processing*, vol. 2008, Feb 2008, Article ID 765615.
- [47] A. Bell and T. Sejnowski, "An information-maximization approach to blind separation and blind deconvolution," *Neural Computation*, vol. 7, no. 6, pp. 1129–1159, 1995.
- [48] S. Amari, A. Cichocki, and H. H. Yang, "A new learning algorithm for blind signal separation," in *Proceedings of Neural Information Processing Systems*, 1996, pp. 757–763.
- [49] J. F. Cardoso and B. H. Laheld, "Equivariant adaptive source separation," *IEEE Transactions on Signal Processing*, vol. 44, no. 12, pp. 3017–3030, Dec 1996.
- [50] S. C. Douglas and M. Gupta, "Scaled natural gradient algorithms for instantaneous and convolutive blind source separation," in 2007 IEEE International Conference on Acoustics, Speech and Signal Processing ICASSP '07, vol. 2, April 2007, pp. II–637–II–640.
- [51] D. Lahat and C. Jutten, "Joint independent subspace analysis using second-order statistics," *IEEE Transactions on Signal Processing*, vol. 64, no. 18, pp. 4891–4904, Sept 2016.
- [52] M. Anderson, G. S. Fu, R. Phlypo, and T. Adalı, "Independent vector analysis: Identification conditions and performance bounds," *IEEE Transactions on Signal Processing*, vol. 62, no. 17, pp. 4399–4410, Sept 2014.

- [53] E. Bingham and A. Hyvärinen, "A fast fixed-point algorithm for independent component analysis of complex valued signals," *International Journal of Neural Systems*, vol. 10, no. 1, pp. 1–8, Feb. 2000.
- [54] P. Tichavský, Z. Koldovský, and E. Oja, "Speed and accuracy enhancement of linear ica techniques using rational nonlinear functions," in *Proceedings of International Conference on Independent Component Analysis and Signal Separation*. Springer Berlin Heidelberg, 2007, pp. 285–292.
- [55] F. Nesta and Z. Koldovský, "Supervised independent vector analysis through pilot dependent components," in 2017 IEEE International Conference on Acoustics, Speech and Signal Processing (ICASSP), March 2017, pp. 536–540.